

Quantum phase transitions in frustrated two-dimensional antiferromagnets

Andrey V. Chubukov^{1,2,3}, Subir Sachdev² and T. Senthil²

¹*Department of Physics, University of Wisconsin, Madison, WI 53706*

²*Departments of Physics and Applied Physics, P.O. Box 208120,
Yale University, New Haven, CT 06520-8120*

and ³*P.L. Kapitza Institute for Physical Problems, Moscow, Russia*

(January 5, 1994)

Abstract

We study frustrated, two-dimensional, quantum antiferromagnets in the vicinity of a quantum transition from a non-collinear, magnetically-ordered ground state to a quantum disordered phase. The general scaling properties of this transition are described. A detailed study of a particular field-theoretic model of the transition, with bosonic spin-1/2 spinon fields, is presented. Explicit universal scaling forms for a variety of observables are obtained and the results are compared with numerical data on the spin-1/2 triangular antiferromagnet. Universal properties of an alternative field-theory, with confined spinons, are also briefly noted.

arXiv:cond-mat/9402006v1 2 Feb 1994

Typeset using REVTeX

I. INTRODUCTION

There has been a remarkable recent revival of interest in the low-energy properties of two-dimensional ($2d$) frustrated quantum antiferromagnets. In part, this interest was triggered by the discovery of strong magnetic fluctuations in the high- T_c superconductors; however, frustrated magnetic systems are interesting in their own right, in the light of numerous theoretical predictions on the nature of disordered ground states in quantum spin systems [1,2,3,4].

Three kinds of frustrated $2d$ systems have been studied intensively, both experimentally and theoretically. First, are antiferromagnets on a triangular lattice such as VCl_2 , VBr_2 , C_6Eu , $NaTiO_2$ etc [5]. Theoretical studies of such antiferromagnets go back to 1973 when Anderson and Fazekas [6] first suggested that for $S = 1/2$, quantum fluctuations may be strong enough to destroy the classical 120° ordering of Heisenberg spins. Though most of the subsequent numerical and analytical studies do indicate [7] the presence of long-range order at zero temperature (T), these studies also show [9] that quantum fluctuations are quite strong.

A second frustrated system is the antiferromagnet on a kagome lattice. It is believed to describe the second layer of 3He on graphite [10] and $SrCr_{8-x}Ga_{4+x}O_{19}$ and related compounds [11]. The effects of quantum fluctuations in kagome antiferromagnets are far stronger than in triangular ones [12], and numerical studies of $S = 1/2$ systems support a quantum-disordered ground state at $T = 0$ [13,9]. Besides, large S kagome antiferromagnets display the Villain order from disorder phenomenon [14]: in the semiclassical approximation, they possess a strong ‘accidental’ degeneracy which is lifted only by the zero-point motion of quantum spins [12,15]. Tunneling between a sequence of nearly degenerate ground states (which differ in energy only due to quantum fluctuations), may also contribute substantially to the reduction in the strength of the large S long-range order [16].

Finally, there are also studies of antiferromagnets on the square lattice which are frustrated by adding second and third neighbor couplings [2,17]. These systems show interesting phases with incommensurate, planar, spiral correlations.

A key feature of the local spin correlations in the systems above, which will be crucial in our analysis, is that they are *non-collinear*. Unlike the unfrustrated square lattice, the spins are not locally either parallel or anti-parallel to one another. The analysis in this paper will mostly assume that the spins are *coplanar* although this second restriction is mostly in the interests of simplicity.

So far we have discussed the situation at $T = 0$. Experiments, however, are performed at finite T when thermal fluctuations are also present. The effects of thermal fluctuations for $2d$ Heisenberg systems are well known [19] - they destroy long-range magnetic correlations at arbitrary small T . Suppose, first, that the ground state is nearly perfectly ordered. It is clear, then, that at small T , thermal fluctuations will be significantly more important than quantum fluctuations, and the low- T behavior will be predominantly classical - the primary effect of quantum fluctuations will be a renormalization of the couplings at $T = 0$. This is the low- T ‘renormalized-classical’ regime which was studied in detail in Ref [35], and later observed [20] in a number of experiments on undoped square-lattice antiferromagnets at sufficiently low T . Consider, next, the physics when the system is quantum-disordered at $T = 0$. Then all thermally induced fluctuations are suppressed by a (presumed) spin-gap at

low enough temperatures and the low-energy dynamics is purely quantum mechanical - this is the “quantum-disordered” [35] regime.

However, there is a third, intriguing possibility which arises when the ground state of the system is not too far from a $T = 0$, second-order quantum transition between the magnetically-ordered and quantum disordered states. Then it is easily possible to find the so-called “quantum-critical” regime where classical and thermal fluctuations are equally important. This is a high temperature regime with respect to any energy-scale which measures the deviation of the ground state of the antiferromagnet from the quantum transition point; on the magnetically-ordered side a convenient choice for this energy-scale is a spin stiffness, ρ_s . However it is also a low temperature regime with respect to a microscopic, short-distance energy scale like a nearest-neighbor exchange constant, J . If the couplings are precisely critical, then the quantum-critical region stretches down to lowest T - this is unlikely to be realized in antiferromagnets without fine-tuning of an external parameter *e.g.* pressure or doping. However, even if the system is not precisely at the critical point, but T is larger than ρ_s on the ordered side, or a corresponding energy scale Δ on the disordered side, we still observe essentially quantum-critical behavior because at such T we effectively probe the system at scales where it does not know on which side of the transition it will end up in its ground state. However, if the long-range order at $T = 0$ is very well established (or, if on the quantum-disordered side, Δ is very large) the condition $k_B T > \rho_s$ ($k_B T > \Delta$) for quantum-criticality may conflict or interfere with $k_B T < J$ and the quantum-critical behavior can be overshadowed by nonuniversal short-range fluctuations. Thus we require that ρ_s (Δ) be reasonably small, and then then we may expect to observe quantum-critical behavior at T smaller than J .

In a recent publication with J. Ye [25], two of us considered whether a quantum-critical region exists in the square-lattice $S = 1/2$ antiferromagnet. We computed various experimentally measurable quantities such as the uniform susceptibility, the correlation length, the dynamic structure factor, and the spin-lattice relaxation rate for antiferromagnets with collinear spin correlations. We found reasonable agreement between the quantum-critical results and the experimental data [20] on $La_{2-x}Sr_xCuO_4$ and with numerical results on $S = 1/2$ antiferromagnets [21]. We argued, therefore, that this system is quantum-critical at intermediate temperatures. In frustrated $2d$ systems, quantum fluctuations are likely to be far stronger. It is therefore reasonable to expect that quantum-critical behavior may be observed in frustrated systems as well. In the present paper, we will present detailed predictions about the quantum-critical properties of frustrated antiferromagnets with non-collinear correlations, to help elucidate this possibility.

The study of quantum-critical behavior is not the only purpose of our analysis. We will also consider the behavior of various observables in the renormalized-classical region. Previous studies in this region were performed by Azaria *et. al.* [18], who focused on a renormalization group analysis for the correlation length. Below, we present, for the first time, expressions for the uniform susceptibility and dynamic structure factor of renormalized-classical, non-collinear antiferromagnets.

An important issue, which makes a study of non-collinear antiferromagnets considerably more difficult than collinear ones, is that the nature of the quantum-disordered phase and the universality of the transition are not well established. The large- N $Sp(N)$ theories [2,22] have argued that the quantum-disordered phase of non-collinear antiferromagnets has deconfined,

spin-1/2, bosonic spinons. In this paper, we derive a macroscopic field-theoretical model which has the same behavior, and study the universality class of the transition between a quantum-disordered phase with deconfined spinons and the magnetically ordered state. We find, quite generally, that such a transition is in the universality class of the $O(4)$ -vector model in spacetime dimension $D = 3$. This result agrees with the semiclassical renormalization group analysis of the magnetically ordered side in $D = 2 + \epsilon$ dimensions of Azaria *et. al* [18]. We will then go on to determine numerous universal, finite temperature properties of such antiferromagnets. These properties have many striking differences from those of the collinear antiferromagnets [25] which possessed confined spinons. Note however, there are other treatments of the transition in non-collinear antiferromagnets [28] which do not have $O(4)$ exponents at $D = 3$. We will review these in Appendix A and show that they in fact have confined spinons. The universal magnetic properties of these approaches differ only in a minor way from those of Ref [25] and will therefore not be discussed in any detail.

We will begin in Section IA by defining carefully, and with considerable generality, the order parameter of coplanar antiferromagnets [23,26,18]. We will also express the staggered dynamic susceptibility in terms of correlations of the order parameter. We will continue our general discussion in Section IB where we will present universal scaling forms for nearly-critical coplanar antiferromagnets. These scaling forms follow from not much more than the presence of hyperscaling and a dynamic critical exponent $z = 1$. On the magnetically-ordered side, the entire dynamic staggered and uniform susceptibilities will be argued to be fully universal functions of five parameters characterizing the ground state: N_0 , the order-parameter condensate, the two stiffnesses ρ_{\parallel} , ρ_{\perp} and the two susceptibilities χ_{\parallel} , χ_{\perp} (defined more precisely below). Similar results will hold also on the quantum disordered side. We emphasize that none of the results of these two sections make any specific assumptions on the universality class of the transition.

In Sections II-VI we will present explicit computations of the universal scaling functions using a particular (we think likely) field-theoretic model of the transition. This approach has deconfined spin-1/2 spinon excitations in the quantum disordered phase, which lead to many interesting observable consequences. Section VII will compare some of the above results with available numerical results for the $S = 1/2$ triangular Heisenberg antiferromagnet; this comparison will use some new results on the $1/S$ expansion of this model which are obtained in Appendix B.

Our main conclusions will be reiterated in Section VIII. The contents of Appendix A were noted above, and some technical details will be presented in Appendix C.

A. Order parameter and other observables

For simplicity, we will restrict our discussion to antiferromagnets with Hamiltonians of the following form:

$$\mathcal{H} = \sum_{i < j} J_{ij} \mathbf{S}_i \cdot \mathbf{S}_j \quad (1.1)$$

where the \mathbf{S}_i are spin S operators on the sites i, j of a regular two-dimensional lattice, and the J_{ij} are the exchange integrals. The J_{ij} respect the symmetries of the lattice, and

are short-ranged, although not necessarily nearest neighbor. The strength of the quantum fluctuations will depend on the value of S and on the ratios of the J_{ij} , and will determine whether the ground state is magnetically ordered or quantum disordered.

In the following, it will be convenient to think of the \mathbf{S}_i not as quantum operators, but as spacetime-dependent fields in a path integral over imaginary time τ . We will restrict our analysis to antiferromagnets in which the strongest fluctuations are well described by the following hydrodynamic parametrization

$$\mathbf{S}_i(\tau) = \mathbf{n}_1(\mathbf{x}_i, \tau) \cos(2\mathbf{Q} \cdot \mathbf{x}_i) + \mathbf{n}_2(\mathbf{x}_i, \tau) \sin(2\mathbf{Q} \cdot \mathbf{x}_i) \quad (1.2)$$

where $\mathbf{n}_1, \mathbf{n}_2$ vary slowly on the scale of a lattice spacing, but are always orthogonal: $\mathbf{n}_1 \cdot \mathbf{n}_2 = 0$ for all \mathbf{x}_i, τ . The ordering wavevector $2\mathbf{Q}$ may be commensurate or incommensurate with reciprocal lattice vectors, but must not be such that (1.2) makes all the \mathbf{S}_i collinear with each other. Thus the square lattice with $2\mathbf{Q} = (\pi, \pi)/a$ is excluded (a is the nearest neighbor spacing), as is any ferromagnetic state ($\mathbf{Q} = 0$). The triangular lattice and certain kagome lattice antiferromagnets with $2\mathbf{Q} = (8\pi/3, 8\pi/\sqrt{3})/a$, or square lattice antiferromagnets with incommensurate \mathbf{Q} are however included. Kagome antiferromagnets with more complicated local correlations, which are nevertheless coplanar, will also be described by our universal results, but are not considered explicitly for simplicity. The parametrization (1.2) also implies that the spin orientations are always locally coplanar. In fact, even antiferromagnets with non-coplanar correlations can be analyzed by a straightforward extension (not described here) of our results. The key restriction is that the correlations are non-collinear: we however assume coplanarity for simplicity.

As is well-known [23,24,26], we can identify the pair of vectors $\mathbf{n}_1, \mathbf{n}_2$ as the order parameter of the antiferromagnet; below we will discuss an equivalent complex matrix order parameter, $Q_{\alpha,\beta}$, which is computationally somewhat more convenient. On the magnetically ordered there will be a spin-condensate which, we assume, satisfies

$$N_0^2 = \langle \mathbf{n}_1 \rangle_{T=0}^2 = \langle \mathbf{n}_2 \rangle_{T=0}^2 \quad (1.3)$$

Our analysis will rely heavily on a spinor parametrization of the vectors $\mathbf{n}_1, \mathbf{n}_2$. This is most directly introduced by the Schwinger boson representation of the spin operators

$$S_a = \frac{1}{2} b_\alpha^\dagger \sigma_{\alpha\beta}^a b_\beta \quad (1.4)$$

where $a = x, y, z$, $\alpha, \beta = 1, 2$, and the σ^a are the Pauli matrices; site and time dependence of the fields is implicit. It turns out that the hydrodynamic form (1.2) is related to the following parametrization of the b :

$$b_{\alpha i}(\tau) = \sqrt{\frac{SZ_S}{2}} \left(z_\alpha(\mathbf{x}_i, \tau) e^{i\mathbf{Q} \cdot \mathbf{x}_i} + i\varepsilon_{\alpha\beta} z_\beta^*(\mathbf{x}_i, \tau) e^{-i\mathbf{Q} \cdot \mathbf{x}_i} \right) \quad (1.5)$$

where ε is the antisymmetric tensor and the z_α are slowly varying complex fields satisfying the following normalization at some scale Λ :

$$\sum_{\alpha=1}^N |z_\alpha|^2 = N \quad (1.6)$$

with $N = 2$ (we have introduced the variable N in anticipation of the generalization below to arbitrary N). The renormalization factor Z_S accounts for the fluctuations at scales shorter than Λ . Inserting (1.5) in (1.4) and comparing with (1.2) we obtain

$$n_{2a} + in_{1a} = \frac{SZ_S}{2} \varepsilon_{\alpha\gamma} z_\gamma \sigma_{\alpha\beta}^a z_\beta \quad (1.7)$$

It is easy to check that this satisfies $\mathbf{n}_1 \cdot \mathbf{n}_2 = 0$ and (1.3). Notice that order parameter fields are *quadratic* in z , this is consistent with the identification of the z quanta as $S = 1/2$ bosonic spinons. The composite character of the order parameter was also noticed (for $N = 2$) in Ref. [29].

Some key properties of the above parametrization deserve notice. First, the question of gauge invariance. As is well-known, the Schwinger boson decomposition (1.4) demands that the physics be invariant under the $U(1)$ gauge transformation $b \rightarrow e^{i\phi} b$. However the continuum parametrization (1.5) ‘breaks’ this gauge symmetry [2]. Alternatively stated, if the z fields are slowly varying in one particular choice of gauge for the b , they will have forbidden rapid variations for most other gauges. Thus, simply by focusing on a long-wavelength theory of the z , we have ‘broken’ the gauge symmetry. There is however, a remnant Z_2 gauge symmetry [2] that must be kept track of: notice that the transformation

$$z(\mathbf{x}, \tau) \rightarrow \eta(\mathbf{x}, \tau) z(\mathbf{x}, \tau) \quad : \quad \eta = \pm 1 \quad (1.8)$$

leaves all the spin operators invariant. All observables must be invariant under this Z_2 gauge transformation. All of these features are consistent with earlier large N theories of frustrated antiferromagnets [2] which found breaking of $U(1)$ gauge invariance down to Z_2 in all non-collinear antiferromagnets.

Consider, next, the symmetries any effective action for the z must satisfy. It must clearly be invariant under any global $SU(2)$ spin rotation $z \rightarrow Uz$, where U is an $SU(2)$ matrix. More interesting, however, is the behavior under lattice translations [29], $\mathbf{x} \rightarrow \mathbf{x} + \mathbf{y}$. The spin-rotation invariance of \mathcal{H} and the parametrization (1.5) are consistent with this only if the action is invariant under the global transformation

$$z \rightarrow e^{-i\mathbf{Q}\cdot\mathbf{y}} z \quad (1.9)$$

where \mathbf{y} is any near-neighbor vector. For the triangular lattice, this demands that the action be invariant under the Z_3 symmetry [29] $z \rightarrow \exp(\pm i2\pi/3)z$, while for incommensurate spiral states it is effectively equivalent to a global $U(1)$ symmetry. In practice we will find that the consequences of the Z_3 symmetry are essentially identical to the larger $U(1)$ symmetry, and we will therefore simply refer to this lattice symmetry as a $U(1)$ symmetry. It is important, however, not to confuse this global, lattice, $U(1)$ symmetry, with the $U(1)$ gauge symmetry discussed above. Thus the effective action for the z field should possess a global $SU(2) \times U(1)$ symmetry [29]; for general N this will be a $SU(N) \times U(1)$ symmetry.

An important observable which will characterize the antiferromagnet, is the staggered dynamic susceptibility χ_s defined by

$$\chi_s(k, i\omega_n) \delta_{ab} = \frac{v_s}{N_s \hbar} \sum_{i,j} \int_0^{\hbar/k_B T} d\tau \langle S_{ia}(\tau) S_{jb}(0) \rangle \exp[-i((\mathbf{k} + 2\mathbf{Q}) \cdot (\mathbf{x}_i - \mathbf{x}_j) - \omega_n \tau)] \quad (1.10)$$

at the small momentum \mathbf{k} away from $2\mathbf{Q}$ and Matsubara frequency ω_n . The sums over i, j extend over all the N_s sites of the system, and v_s is the volume per spin (e.g., $v_s = a^2\sqrt{3}/2$ for triangular antiferromagnet).

The physically measurable retarded staggered susceptibility can of course be obtained by the usual analytic continuation to real frequencies. Inserting (1.4) and (1.5) in (1.10), we find

$$\chi_s(k, i\omega_n) = \frac{1}{N(N+1)\hbar} \sum_{\alpha, \beta=1}^N \int d^2x \int_0^{\hbar/k_B T} d\tau \langle Q_{\alpha\beta}(\mathbf{x}, \tau) Q_{\alpha\beta}^*(0, 0) \rangle e^{-i(\mathbf{k}\cdot\mathbf{x} - \omega_n\tau)} \quad (1.11)$$

where $N = 2$, and the symmetric order-parameter $Q_{\alpha\beta} = Q_{\beta\alpha}$ is given by

$$Q_{\alpha\beta} = \frac{SZ_S}{N} z_\alpha z_\beta. \quad (1.12)$$

Note that it has $N(N+1)/2$ different complex components, and is invariant under the Z_2 gauge transformation (1.8). It transforms under $SU(N) \times U(1)$ as a 1×2 Young tableau under $SU(N)$ and as charge 2 under $U(1)$. Again we have introduced an N -dependent notation to facilitate the generalization to arbitrary N . The equation (1.3) for the magnitude of the order parameter can also be expressed in the general form

$$N_0^2 = \sum_{\alpha\beta=1}^N \left| \langle Q_{\alpha\beta} \rangle_{T=0} \right|^2 \quad (1.13)$$

We also quote for reference the relationship, special to $N = 2$, between the tensor order parameter $Q_{\alpha\beta}$ and the vectors $\mathbf{n}_1, \mathbf{n}_2$, which can be deduced from (1.7) and (1.12):

$$Q = \frac{1}{2} \begin{pmatrix} -n_{2x} + in_{2y} - in_{1x} - n_{1y} & n_{2z} + in_{1z} \\ n_{2z} + in_{1z} & n_{2x} + in_{2y} + in_{1x} - n_{1y} \end{pmatrix} \quad (1.14)$$

We will find it convenient to express many of our results in terms of the dynamic, staggered, structure factor which is the Fourier transform of the spin-spin correlation function in real time t

$$S(k, \omega) \delta_{l,m} = \int d^2x \int_{-\infty}^{\infty} dt \langle S_l(\mathbf{x}, t) S_m(0, 0) \rangle \exp -i(\mathbf{k}\mathbf{x} - \omega t) \quad (1.15)$$

This is of course related to the staggered susceptibility defined above by

$$S(k, \omega) = \frac{2\hbar}{1 - e^{-\hbar\omega/(k_B T)}} \text{Im} \chi_s(k, \omega) \quad (1.16)$$

In addition to the order parameter, the uniform magnetization density, $\mathbf{M}(\mathbf{x})$, is an important hydrodynamic variable. Its fluctuations decay slowly due to the conservation law for the total magnetization. It is defined by

$$\mathbf{M}(\mathbf{x}_i, t) = \frac{g\mu_B}{v_s} \mathbf{S}_i(t), \quad (1.17)$$

where $g\mu_B/\hbar$ is the hydromagnetic ratio. Its diffusion is measured by the uniform spin susceptibility defined by

$$\chi_u(k, \omega) \delta_{ab} = -\frac{i}{\hbar} \int d^2x \int_0^{\infty} dt \langle [M_a(\mathbf{x}, t), M_b(0, 0)] \rangle \exp -i(\mathbf{k}\mathbf{x} - \omega t) \quad (1.18)$$

B. Scaling forms

We will now consider the properties of the non-collinear antiferromagnets in the vicinity of a second-order quantum phase transition from a magnetically ordered to a quantum disordered ground state. We will try to keep the discussion in this section as general as possible, independent of any specific field theory for the transition. The results of this subsection will follow from some fairly general scaling assumptions, rather similar to those applied to collinear antiferromagnets in Ref [25]. A primary assumption will be that the quantum transition has dynamic critical exponent $z = 1$. Explicit computations of the scaling functions and exponents will be performed in the subsequent sections using a particular deconfined-spinon field-theory of the transition. A confined-spinon field-theory will be briefly considered in Appendix A; its properties are also consistent with the scaling ideas of this section.

Let us assume that the $T = 0$ transition occurs as some coupling constant g is varied through a critical value $g = g_c$, and the magnetically ordered state occurs for $g < g_c$.

We present first the scaling properties for $g < g_c$. We expect that the condensate N_0 will vanish as

$$N_0 \sim (g_c - g)^{\bar{\beta}} \quad (1.19)$$

where $\bar{\beta}$ is a universal critical exponent. A second characterization of the ordered ground state is provided by the spin stiffnesses ρ_{\parallel} and ρ_{\perp} : these measure the energy cost of twists in the plane and perpendicular to the plane of the order parameter, respectively. In the presence of hyperscaling (which we assume), we expect that both these stiffnesses will vanish as

$$\rho_{\perp}, \rho_{\parallel} \sim (g_c - g)^{\nu} \quad (1.20)$$

where the ν is the usual correlation length exponent (this formula is special to two dimensions). Further, the ratio of these two stiffnesses will obey

$$\lim_{g \nearrow g_c} \frac{\rho_{\parallel}}{\rho_{\perp}} = \Upsilon_{\rho} \quad (1.21)$$

where Υ_{ρ} is a *universal* number. In a similar manner we can consider the two uniform magnetic susceptibilities χ_{\parallel} , χ_{\perp} defining the response of the antiferromagnet with infinitesimal anisotropy to uniform magnetic fields perpendicular and parallel to the plane of the order parameter, respectively (note the inversion in the order of ‘parallel’ and ‘perpendicular’!). In a $z = 1$ theory their scaling properties are identical to those of the spin stiffnesses, and possess an associated universal ratio Υ_{χ} . The subsequent sections of this paper consider a field theory in which $\Upsilon_{\rho} = \Upsilon_{\chi} = 1$ exactly; in Appendix A we briefly consider a model with different universal ratios. In all cases it is useful to consider the dimensionless numbers y_{ρ} , y_{χ}

$$y_{\rho} = \frac{\rho_{\parallel} - \Upsilon_{\rho}\rho_{\perp}}{\rho_{\perp}} \quad ; \quad y_{\chi} = \frac{\chi_{\parallel} - \Upsilon_{\chi}\chi_{\perp}}{\chi_{\perp}} \quad (1.22)$$

which measure the deviation of the stiffnesses and susceptibilities from the universal ratio at the critical point; clearly $y_{\rho}, y_{\chi} \rightarrow 0$ as $g \rightarrow g_c$. Finally, as in Ref [25], we also need

the following dimensionless ratios which measure the wavevector, frequency, and stiffness in units of the absolute temperature

$$\bar{k} = \frac{\hbar c_{\perp} k}{k_B T} ; \quad \bar{\omega} = \frac{\hbar \omega}{k_B T} ; \quad x_1 = \frac{N k_B T}{4\pi \rho_{\perp}} ; \quad (1.23)$$

The numerical factor of 4π is for future notational convenience, and the spin-wave velocities c_{\perp} , c_{\parallel} are of course given by $c_{\perp}^2 = \rho_{\perp}/\chi_{\perp}$ and $c_{\parallel}^2 = \rho_{\parallel}/\chi_{\parallel}$. The factor N in x_1 has been inserted because $\rho_{\perp} \propto N$ in the large limit, and so ensures that x_1 remains of order unity in this limit.

Now, following arguments closely related to those in Ref. [25], we may conclude that the response functions of nearly-critical antiferromagnets obey the following universal scaling forms

$$\chi_s(k, \omega) = \frac{2\pi N_0^2}{N \rho_{\perp}} \left(\frac{N k_B T}{4\pi \rho_{\perp}} \right)^{\bar{\eta}} \left(\frac{\hbar c_{\perp}}{k_B T} \right)^2 \Phi_{1s}(\bar{k}, \bar{\omega}, x_1, y_{\rho}, y_{\chi}) \quad (1.24)$$

$$\chi_u(k, \omega) = \left(\frac{g \mu_B}{\hbar c_{\perp}^2} \right)^2 k_B T \Phi_{1u}(\bar{k}, \bar{\omega}, x_1, y_{\rho}, y_{\chi}) \quad (1.25)$$

$$S(k, \omega) = \frac{2\pi \hbar N_0^2}{N \rho_{\perp}} \left(\frac{N k_B T}{4\pi \rho_{\perp}} \right)^{\bar{\eta}} \left(\frac{\hbar c_{\perp}}{k_B T} \right)^2 \frac{2}{1 - e^{-\bar{\omega}}} \Xi_1(\bar{k}, \bar{\omega}, x_1, y_{\rho}, y_{\chi}) \quad (1.26)$$

Here Φ_{1s} , Φ_{1u} and Ξ_1 are completely universal functions of their dimensionless arguments and there are no non-universal scale factors anywhere. The exponent $\bar{\eta}$ is related to the order parameter exponent $\bar{\beta}$ by the hyperscaling relation

$$2\bar{\beta} = (1 + \bar{\eta})\nu. \quad (1.27)$$

From the above scaling relation and (1.19) and (1.20) we see that the prefactors of all the scaling functions remain finite all the way up-to $g = g_c$, or $x_1 = \infty$. Further, all scaling functions are defined such that they remain finite as $x_1 \rightarrow \infty$ when we will also find $y_{\rho, \chi} \rightarrow 0$. The universal functions Φ_{1s} and Ξ_1 are related by the fluctuation-dissipation theorem $\Xi_1 = \text{Im}\Phi_{1s}$. As in [25], the argument x_1 determines whether the system is better described at large scales by a quantum-critical ($x_1 \gg 1$) or a renormalized-classical ($x_1 \ll 1$) theory.

Strictly speaking, the leading scaling properties of the observables are obtained at $y_{\rho} = y_{\chi} = 0$, because these ratios are associated with irrelevant operators. However many long-distance properties are sensitive to the precise values of the spin-stiffnesses and susceptibilities. Thus these operators are actually *dangerously irrelevant*, and it necessary to consider many observables as full functions of y_{ρ} and y_{χ} .

Parallel arguments can be applied to the quantum disordered state with $g > g_c$. We assume that this state has low-lying quasiparticle excitations with non-zero spin, characterized by an energy scale Δ , which propagate with a velocity c . In the model considered in the subsequent sections we will have spin-1/2, bosonic quasiparticles above a gap Δ ; there are however other possibilities, one of which is discussed in Appendix A. We expect that Δ will obey

$$\Delta \sim (g - g_c)^\nu \quad (1.28)$$

near the critical point. We also introduce the dimensionless ratio

$$x_2 = \frac{k_B T}{\Delta} \quad (1.29)$$

which is the analog of the x_1 on the ordered side. There is now no need to consider the analogs of the y_ρ, y_χ as these will be truly irrelevant (as opposed to dangerously irrelevant) on the disordered side. The observables of the nearly-critical, quantum-disordered antiferromagnet obey

$$\chi_s(k, \omega) = \mathcal{A} \left(\frac{\hbar c}{k_B T} \right)^2 \left(\frac{k_B T}{\Delta} \right)^{\bar{\eta}} \Phi_{2s}(\bar{k}, \bar{\omega}, x_2) \quad (1.30)$$

$$\chi_u(k, \omega) = \left(\frac{g\mu_B}{\hbar c^2} \right)^2 k_B T \Phi_{2u}(\bar{k}, \bar{\omega}, x_2) \quad (1.31)$$

$$S(k, \omega) = \hbar \mathcal{A} \left(\frac{\hbar c}{k_B T} \right)^2 \left(\frac{k_B T}{\Delta} \right)^{\bar{\eta}} \frac{2}{1 - e^{-\bar{\omega}}} \Xi_2(\bar{k}, \bar{\omega}, x_2) \quad (1.32)$$

Again Φ_{2s}, Φ_{2u} and Ξ_2 are completely universal functions. The prefactor \mathcal{A} is related to quasiparticle amplitude(s) and vanishes as

$$\mathcal{A} \sim (g - g_c)^{\bar{\eta}\nu} \quad (1.33)$$

The precise definition of \mathcal{A} requires a normalization condition on Φ_{2s} which will be discussed later.

Before closing this section, we briefly introduce the scaling functions of some other important observables which can be deduced from the ones above. We restrict ourselves to the ordered side; the extension to the disordered side is straightforward. The scaling function for the spin correlation length is

$$\xi^{-1} = \frac{k_B T}{\hbar c_\perp} X(x_1, y_\rho, y_\chi) \quad (1.34)$$

The static uniform spin susceptibility at $g < g_c$ behaves as

$$\chi_u(T) = \left(\frac{g\mu_B}{\hbar c_\perp} \right)^2 k_B T \Omega(x_1, y_\rho, y_\chi) \quad (1.35)$$

The local structure factor $S_L(\omega)$ is given by $S_L(\omega) = \int d^2k S(k, \omega)/4\pi^2$. The contribution of χ_u to $S_L(\omega)$ is subdominant and S_L is given simply by a momentum integral of the staggered susceptibility. This integral is always ultraviolet convergent (because the intermediate states in $S(k, \omega)$ are all on-shell) and is dominated by \bar{k} less than about 1; we have therefore

$$S_L(\bar{\omega}) = \frac{2\pi\hbar N_0^2}{N\rho_\perp} \left(\frac{Nk_B T}{4\pi\rho_\perp} \right)^{\bar{\eta}} \frac{2}{1 - e^{-\bar{\omega}}} K_1(\bar{\omega}, x_1, y_\rho, y_\chi) \quad (1.36)$$

where $K_1 = \int d^2\bar{k} \Xi_1/4\pi^2$. The small frequency limit of $S_L(\omega)$ is directly related to the spin-lattice relaxation rate $1/T_1 \propto S_L(\bar{\omega} \rightarrow 0)$. We will also discuss static structure factor

$S(k) = \int d\omega S(k, \omega) / 2\pi$. The frequency integral is divergent at the upper cutoff if $\bar{\eta} > 1$, whence $S(k)$ is non-universal - this will be the case in our model.

In the subsequent sections we will obtain explicit expressions for the scaling functions introduced above in the renormalized-classical and quantum-critical regions. We will use a new deconfined spinon field theory which will be introduced in Section II, along with a $1/N$ expansion which will facilitate our computations. Properties of the quantum-disordered phase will also be discussed.

II. EFFECTIVE FIELD THEORY: DECONFINED SPINONS

The main aim of the remainder of this paper is to illustrate the general scaling ideas discussed above in the framework of a specific field theoretical model of the quantum transition. An important property of field-theory we use is that results of the $1/N$, spacetime $D = 4 - \epsilon$, and $D = 2 + \epsilon$, expansions on it are *all* consistent with each other; we will consider only the $1/N$ expansion here.

A significant reason behind the choice of our particular model is that it possesses deconfined spin-1/2 spinon excitations in the quantum disordered state. This is then consistent with the $Sp(N)$ -large N prediction of Ref. [2] on non-collinear antiferromagnets. Further, our approach will allow us to explore some of the observable consequences of these novel excitations.

We begin with some discussion on the role of the Z_2 gauge symmetry of (1.8). The crucial role of this gauge symmetry was noted in was emphasized to us at an early stage by N. Read [32] and was also noted in Ref [2]. Our main assumption will be that the Z_2 gauge symmetry can be entirely neglected in the continuum field theory. In other words, configurations with a non-zero local Z_2 flux remain gapful across the transition. The Z_2 gauge fluxes are in fact present in the cores of vortex lines (in spacetime) associated with homotopy group $\pi_1(SO(3)) = Z_2$ of the true $SO(3)$ order parameter [31]. We assume that these vortices remain confined across the transition and that the Z_2 gauge charge of the z field is globally defined [32] (the z -field configuration around a vortex is double-valued). Under these circumstances we may simply write down a continuum Landau-Ginzburg field theory for the z -field. Implicitly, this procedure implies that we are not distinguishing between $SU(2)$ and $SO(3)$ symmetries.

We will now write down the most general action consistent with the $SU(N) \times U(1)$ symmetry discussed before. Rather than using a soft-spin Landau-Ginzburg approach, we find it more convenient to use hard spins satisfying (1.6); this modification is however not crucial and completely equivalent results can be obtained by the former approach. To second-order in spatial gradients this yields the following effective action

$$\mathcal{S} = \int d^2x d\tau \sum_{\mu=\vec{x}, \tau} \frac{1}{g_\mu} \left[\partial_\mu z_\alpha^* \partial_\mu z_\alpha - \frac{\gamma_\mu}{4N} (z_\alpha^* \partial_\mu z_\alpha - \partial_\mu z_\alpha^* z_\alpha)^2 \right]. \quad (2.1)$$

where $\alpha = 1 \dots N$, and $g_x, g_\tau, \gamma_x, \gamma_\tau$ are coupling constants. Any of these couplings can be varied to tune through the quantum transition - we will use

$$g \equiv g_x. \quad (2.2)$$

Simple considerations presented in Section III below show that these coupling constants are given by

$$g_x = \frac{N}{2\rho_{\perp}^0}, \quad g_{\tau} = \frac{N}{2\chi_{\perp}^0}, \quad \gamma_x = \frac{\rho_{\parallel}^0 - \rho_{\perp}^0}{\rho_{\perp}^0}, \quad \gamma_{\tau} = \frac{\chi_{\parallel}^0 - \chi_{\perp}^0}{\chi_{\perp}^0}, \quad (2.3)$$

and ρ^0 and χ^0 are the bare values of two spin stiffnesses and spin susceptibilities. For simplicity, throughout the paper we define transverse and longitudinal susceptibility without a factor $g\mu_B/\hbar$. A more detailed consideration of the values of ρ , χ is presented in the next section.

The effective action \mathcal{S} can also be explicitly derived from microscopic considerations. Using the continuum parametrization in (1.5) it is not difficult to show that the long-distance limit of the $Sp(N)$ theories of Refs [2] and [12] is described precisely by \mathcal{S} . The same parametrization can also be used on the semiclassical approach of [26] to obtain \mathcal{S} . Finally, we also explicitly derived the effective action (2.1) for $N = 2$ from the general macroscopic approach of Ref [23].

Some critical properties of \mathcal{S} can be immediately deduced. By a simple power-counting argument in $D = 4 - \epsilon$ dimensions it can be shown that the γ_{μ} couplings are irrelevant at the critical point. An identical result can also be obtained by $D = 2 + \epsilon$ analysis parallel to that of Ref [18]. We will also explicitly show the irrelevancy of the γ_{μ} in the $1/N$ expansion below. (None of these arguments of course exclude the possibility that a large bare value of γ_{μ} may have more fundamental effects. In fact, at $\gamma_{\mu} = -N$, \mathcal{S} actually becomes the $U(1)$ gauge invariant CP^{N-1} model, which is then a model for quantum phase transitions in collinear antiferromagnets. We will not consider the possibility of these large γ_{μ} complications in this paper.)

It is therefore useful to begin the analysis by considering \mathcal{S} at $\gamma_{\mu} = 0$. It is easy to verify that now \mathcal{S} has its internal symmetry enlarged from $SU(N) \times U(1)$ to $O(2N)$. Further, the spacetime theory is Lorentz invariant. Finally, this theory has $\rho_{\parallel} = \rho_{\perp}$ (and similarly for χ) and so we have $\Upsilon_{\rho} = \Upsilon_{\chi} = 1$ exactly

The exponents appearing in the scaling functions are now all properties of the well-known $O(2N)$ fixed point, and we quote for reference to order $1/N$ (see also Appendix C)

$$\nu = 1 - \frac{16}{3\pi^2 N}; \quad \bar{\eta} = 1 + \frac{32}{3\pi^2 N}; \quad \bar{\beta} = 1 + \mathcal{O}(1/N^2) \quad (2.4)$$

Note that the exponents $\bar{\eta}$ and $\bar{\beta}$ are associated with the composite field $Q_{\alpha\beta}$ and thus differ from the usual η , β for vector fields. Thus $\bar{\eta}$ is quite close to unity at large N , while the corresponding η which appears in collinear antiferromagnets is almost zero.

Let us now consider how the γ_{μ} variables break the Lorentz and $O(2N)$ symmetry. Tedious but straightforward computations show that the terms proportional to the γ_{μ} transform under a single irreducible representation of $O(2N)$ - the one labeled by a Young tableau of 2 rows and 2 columns. It is therefore not necessary to decompose the $O(2N)$ structure of the operator. However the γ_{μ} terms are irreducible under the Lorentz group - there are the spin-0 and spin-2 pieces

$$\begin{aligned} \gamma_1 &= (2\gamma_x + \gamma_{\tau})/3 \\ \gamma_2 &= (\gamma_x - \gamma_{\tau})/3. \end{aligned} \quad (2.5)$$

The terms associated with the γ_1 and γ_2 are now completely irreducible under $O(2N)$ and Lorentz group, and will therefore have their independent crossover exponents, ϕ_1 and ϕ_2 respectively, measuring their irrelevancy. In other words, near the quantum fixed point, the fully renormalized spin stiffnesses and susceptibilities should obey

$$\begin{aligned}\frac{\rho_{\parallel} - \rho_{\perp}}{\rho_{\perp}} &= \gamma_1(\xi_J)^{-\phi_1} + \gamma_2(\xi_J)^{-\phi_2} \\ \frac{\chi_{\parallel} - \chi_{\perp}}{\chi_{\perp}} &= \gamma_1(\xi_J)^{-\phi_1} - 2\gamma_2(\xi_J)^{-\phi_2}\end{aligned}\quad (2.6)$$

where ξ_J is the Josephson correlation length measured in lattice units. To leading order in γ we also have from (2.6) for the spin-wave velocity difference,

$$\frac{c_{\parallel} - c_{\perp}}{c_{\perp}} = \frac{3}{2} \gamma_2(\xi_J)^{-\phi_2}\quad (2.7)$$

As g_{μ} approaches g_{μ}^c , ξ_J behaves as $\xi_J \sim (1 - g_{\mu}/g_{\mu}^c)^{-\nu}$ (clearly, $g_x/g_x^c = g_{\tau}/g_{\tau}^c$). In section III we will find the following $1/N$ expansion result for the renormalization-group eigenvalues attracting the $\gamma_{1,2}$ to the fixed point

$$\phi_1 = 1 + \frac{32}{3\pi^2 N} \quad ; \quad \phi_2 = 1 + \frac{112}{15\pi^2 N}\quad (2.8)$$

III. CONSERVED CHARGES AND CURRENTS

This section will present the computation of the spin stiffnesses and uniform spin susceptibilities both at $T = 0$ and in the quantum critical region of the deconfined spinon action \mathcal{S} . The calculation will be carried out to order $1/N$. We will show how one can obtain renormalized stiffnesses in the ground state by doing calculations in the symmetric phase at $T \rightarrow 0$. A computation of stiffnesses directly in the ordered phase is performed in the Appendix C.

The stiffnesses and uniform susceptibilities are all response functions associated with the conserved charges and currents of \mathcal{S} . We will therefore begin by studying the $SU(N) \times U(1)$ symmetry of \mathcal{S} . The conserved charges and currents can be determined by the usual procedure of evaluating the change in the action under an infinitesimally small symmetry transformation with a spacetime dependent angle. The results are conveniently expressed in terms of the $N^2 - 1$ traceless Hermitian $SU(N)$ generators T^a which we choose to satisfy

$$\text{Trace}(T^a T^b) = \frac{1}{2} \delta^{ab}\quad (3.1)$$

Then the currents associated with the $SU(N)$ symmetry can be written as

$$K_{\mu}^a = -\frac{i}{g_{\mu}} \left(z^{\dagger} T^a \partial_{\mu} z - \partial_{\mu} z^{\dagger} T^a z \right) - \frac{i\gamma_{\mu}}{Ng_{\mu}} \left(z^{\dagger} \partial_{\mu} z - \partial_{\mu} z^{\dagger} z \right) \left(z^{\dagger} T^a z \right)\quad (3.2)$$

The index μ extends over \vec{x}, τ and K_{τ}^a is, strictly speaking, a conserved charge density - in this section we will use the term ‘current’ to generically refer to both charges and currents.

We will also not explicitly display the spacetime-dependence of the fields. The current associated with the $U(1)$ symmetry is

$$J_\mu = -\frac{i}{g_\mu} (1 + \gamma_\mu) (z^\dagger \partial_\mu z - \partial_\mu z^\dagger z) \quad (3.3)$$

Our intention is to express the fully renormalized stiffnesses in terms of $SU(N)$ and $U(1)$ current-current correlators, and so we need the appropriate Kubo formula. To derive this formula it is convenient to introduce vector potentials which linearly couple to the conserved currents above, and examine the response of the system to these vector potentials. Let us consider first a $SU(N)$ vector potential A_μ^a . This modifies the action to

$$\mathcal{S}' = \frac{1}{g_\mu} \int d^2x d\tau \left[\left| (\partial_\mu + iA_\mu^a T^a) z \right|^2 - \frac{\gamma_\mu}{4N} \left(z^\dagger (\partial_\mu z + iA_\mu^a T^a z) - (\partial_\mu z^\dagger - iA_\mu^a z^\dagger T^a) z \right)^2 \right] \quad (3.4)$$

It is then not difficult to obtain the response of the free energy $F = -\log \left[\int \mathcal{D}z e^{-\mathcal{S}'} \right]$ to the external vector potential. Doing the algebra we find

$$\frac{\delta^2 F}{\delta A_\mu^a \delta A_\mu^b} = -\langle K_\mu^a K_\mu^b \rangle_S + \frac{1}{g_\mu} \langle z^\dagger (T^a T^b + T^b T^a) z \rangle_S + \frac{2\gamma_\mu}{Ng_\mu} \langle z^\dagger T^a z z^\dagger T^b z \rangle_S \quad (3.5)$$

Again space-time dependences have been suppressed, and the two fields inside the correlator are at different spacetime points. A very similar analysis can be carried out for a $U(1)$ vector potential a_μ , and we find

$$\frac{\delta^2 F}{\delta a_\mu^2} = -\langle J_\mu J_\mu \rangle_S + \frac{2N(1 + \gamma_\mu)}{g_\mu} \quad (3.6)$$

Now we change tracks and evaluate the response of the system to these vector potentials in an entirely different way. Let us assume that we are on the ordered side ($g < g_c$), and are able to integrate out all the fluctuations, including the amplitude fluctuation modes in the direction of the condensate. We then obtain a *fully* renormalized action for the spin-wave fluctuations. Let this effective action have the following form

$$F = 2 \int d^2x d\tau \left[\rho_{1\mu} |\partial_\mu Z|^2 - (\rho_{2\mu} - \rho_{1\mu}) (Z^\dagger \partial_\mu Z)^2 \right] \quad (3.7)$$

Here Z is a N -component complex vector of *unit* length which yields the local orientation of the condensate. The factor of 2 in F is introduced for further convenience. Let the condensate point in some fixed direction $Z_0 = (1, 0, 0, 0, \dots)$. We now look at small variations about this direction as in

$$Z = Z_0 + (i\sigma, \pi_1 + i\pi_2, \pi_3 + i\pi_4, \dots)/2; \quad (3.8)$$

the factor of 1/2 is present because Z is a spinor and rotates by only half the angle of the observable order parameter. The effective action for this variation is

$$F = \frac{1}{2} \int d^2x d\tau \left[\rho_{1\mu} \sum_{i=1}^{2N-2} (\partial_\mu \pi_i)^2 + \rho_{2\mu} (\partial_\mu \sigma)^2 \right] \quad (3.9)$$

By the definition of the stiffnesses we identify ρ_{1x}, ρ_{2x} as the two spin stiffnesses of the spin wave modes:

$$\rho_{1x} = \rho_\perp \quad , \quad \rho_{2x} = \rho_\parallel \quad (3.10)$$

Also the stiffness to twists in the time direction gives us the uniform spin susceptibility:

$$\rho_{1\tau} = \chi_\perp \quad , \quad \rho_{2\tau} = \chi_\parallel \quad (3.11)$$

Now let us look at the response of F to the presence of an external $SU(N)$ vector potential, while the condensate is non-zero. Doing the same analysis as before we obtain

$$\delta F = 2 \int d^2x d\tau \left[\rho_{1\mu} A_\mu^a A_\mu^b Z_0^\dagger T^a T^b Z_0 + (\rho_{2\mu} - \rho_{1\mu}) A_\mu^a A_\mu^b \left(Z_0^\dagger T^a Z_0 \right) \left(Z_0^\dagger T^b Z_0 \right) \right] \quad (3.12)$$

For a fixed condensate Z_0 this result will depend upon the orientation of the $SU(N)$ rotation A_μ^a . However if we place the system in a box of large, but finite length L_μ in the μ direction the response of F is clearly proportional to δ^{ab} because no symmetry can be broken (for the case $\mu = \tau$ this equivalent to having a small finite temperature $T \propto L_\tau^{-1}$). Thus we should replace each $T^a T^b$ factor by its average over all the generators of $SU(N)$ - it is crucial that we average over all the generators, and not over different orientations of the condensate. We will then need the identities

$$\begin{aligned} \frac{1}{N^2 - 1} \sum_a Z_0^\dagger T^a T^a Z_0 &= \frac{1}{2N} \\ \frac{1}{N^2 - 1} \sum_a \left(Z_0^\dagger T^a Z_0 \right)^2 &= \frac{1}{2N(N+1)} \end{aligned} \quad (3.13)$$

which are actually true for *any* complex unit vector Z_0 . These identities can be easily established by considering explicit forms for the T^a . So finally, combining (3.12) and (3.13), we can determine the response of F to the $SU(N)$ vector potentials at an infinitesimal temperature:

$$\frac{\delta^2 F}{\delta A_\tau^a \delta A_\tau^b} = \delta^{ab} \frac{2}{N} \frac{N\chi_\perp + \chi_\parallel}{(N+1)} \quad ; \quad \frac{\delta^2 F}{\delta A_x^a \delta A_x^b} = \delta^{ab} \frac{2}{N} \frac{N\rho_\perp + \rho_\parallel}{(N+1)} \quad (3.14)$$

We will evaluate the left-hand side using (3.5) and thence obtain an expression for the above linear combination of the stiffnesses.

We still need a second linear combination - this is of course provided by the $U(1)$ currents. An exactly parallel computation can be done for the response to the $U(1)$ vector potential a_τ - in this case we find

$$\frac{\delta^2 F}{\delta a_\tau^2} = 4\chi_\parallel \quad ; \quad \frac{\delta^2 F}{\delta a_x^2} = 4\rho_\parallel \quad (3.15)$$

Combined with (3.6), (3.5) and (3.6) we now have reduced determination of the spin stiffnesses and susceptibilities to evaluation of the correlators in (3.5), (3.6) at $T = 0$. This calculation will be carried out in Section III A to order $1/N$.

These methods can also be used to obtain the temperature dependence of the uniform spin susceptibility $\chi_u(T)$. By analysis similar to that in Ref [25] it is not difficult to show that

$$\chi_u(T) = \left(\frac{g\mu_B}{\hbar}\right)^2 \frac{\delta^2 F}{\delta A_\tau^a \delta A_\tau^a} \quad (3.16)$$

where there is no summation over a . This computation will be considered in Section III B.

We conclude with a note on the nature of the $1/N$ expansion of \mathcal{S} . We found that a properly renormalized theory for the scaling functions can only be defined if we restrict with the leading terms in an expansion in powers of γ_μ : we shall therefore do a double expansion in powers of $1/N$ and γ_μ . This expansion is most easily done by treating the effects of γ_μ perturbatively - *i.e.* without introducing a Hubbard - Stratonovich decoupling of the quartic term.

A. Spin-stiffnesses and susceptibilities at $T = 0$

Below we will need the form for the vertex function associated with the anisotropic term in the action. In the momentum space we have

$$\Gamma_{\alpha,\beta}(k_{1,\mu}, k_{2,\mu}; k_{3,\mu}, k_{4,\mu}) = \frac{\gamma_\mu}{4N} z_{1,\alpha}^\dagger z_{2,\beta}^\dagger z_{3,\alpha} z_{4,\beta} (k_{1,\mu} + k_{3,\mu})(k_{2,\mu} + k_{4,\mu}) \quad (3.17)$$

where α and β number the components of the z -field. The diagrammatic representation for the current-current correlation functions is shown in Fig.1. At $N = \infty$, one can neglect self-energy and vertex correction within a bubble; however the renormalization due to Γ generally cannot be neglected because the summation over the components of the z -field in the extra bubble associated with Γ yields a factor of N which cancels out the $1/N$ factor in (3.17). However, a simple inspection of the diagrams shows that the effects of Γ are relevant at $N = \infty$ only for the $U(1)$ correlator, while for the $SU(N)$ currents, the side vertices in the bubble contain sign-oscillating T matrices, and the summation over the components of z -field gives only a factor $\mathcal{O}(1)$. As a result, we find at $N \rightarrow \infty$ and in the limit $T \rightarrow 0$

$$2N \frac{\delta^2 F}{\delta A_\mu^a \delta A_\mu^b} = 2N \delta^{ab} \left(\frac{1}{g_\mu} - \frac{1}{g_\mu^c} \right) \quad (3.18)$$

and

$$\frac{\delta^2 F}{\delta a_\mu^2} = 2N \left(\frac{1}{g_\mu} - \frac{1}{g_\mu^c} \right) \left[1 + \gamma_\mu \frac{(g_\mu^c - g_\mu)}{g_\mu^c} \right] \quad (3.19)$$

where $g_x^c = g_c$ and $g_\tau^c = c_\perp^2 g_c$. Clearly from (3.14, 3.15), the r.h.s. in (3.18) and (3.19) are also the values of $4\rho_{\perp\mu}$ and $4\rho_{\parallel\mu}$ respectively. Note that, as one might expect, only ρ_{\parallel}

acquires a correction due to γ , while ρ_{\perp} remains the same as in the isotropic case. Also note that (3.19) is indeed consistent with (2.6) and establishes that $\phi_1 = \phi_2 = 1$ at $N = \infty$.

We now describe the $1/N$ corrections. Obviously, we have to consider the self-energy and vertex corrections within a bubble in Fig.1, and the renormalization of the vertex function Γ itself. The latter however is again relevant only for $U(1)$ response, while for $SU(N)$ response, the leading effect of γ_{μ} is itself of order γ_{μ}/N and there is no need to consider the renormalization of Γ to order $1/N$. The computation of the $SU(N)$ response therefore requires less efforts, and evaluating the diagrams in Fig.1 with Γ given by (3.17), we obtain

$$2N \frac{\delta^2 F}{\delta A_{\mu}^a \delta A_{\mu}^b} = 2N \delta^{ab} \frac{1 + \gamma_{\mu}/(2N)}{g_{\mu}} \left[\left(1 - \frac{g_{\mu}}{\bar{g}_{\mu}^c}\right)^{\nu} + \frac{\gamma_{\mu}}{2N} \left(1 - \frac{g_{\mu}}{\bar{g}_{\mu}^c}\right)^{2\nu} \right] \quad (3.20)$$

where $\bar{g}_{\mu}^c = g_{\mu}^c(1 + \gamma_{\mu}/2N)$ and $\nu = 1 - 16/3\pi^2 N$ is the critical exponent for the correlation length.

Our next step will be to calculate, with logarithmic accuracy, the renormalized value of Γ as $T \rightarrow 0$. We will then use the result to compute the $U(1)$ response to order $1/N$. The diagrams which contribute to the vertex renormalization to order $1/N$ are shown in Fig. 2. The internal part of each diagram contains two Green functions and the polarization operator - this combination produces logarithms after *integration* over intermediate momentum and frequency in 2+1 dimensions [25]. The evaluation of diagrams is tedious but straightforward, and after doing the algebra we obtained that the momentum dependence of the vertex remains the same as in (3.17) but γ_{μ} changes to γ_{μ}^{eff} where

$$\begin{aligned} \gamma_{\tau}^{eff} &= \gamma_{\tau} \left(1 + \frac{128}{15\pi^2 N} \log(1 - g_x/g_c)\right) + \gamma_x \frac{32}{15\pi^2 N} \log(1 - g_x/g_c) \\ \gamma_x^{eff} &= \gamma_x \left(1 + \frac{48}{5\pi^2 N} \log(1 - g_x/g_c)\right) + \gamma_{\tau} \frac{16}{15\pi^2 N} \log(1 - g_x/g_c) \end{aligned} \quad (3.21)$$

Substituting the renormalized vertex into the bubble diagram for $U(1)$ response and performing also self-energy and vertex renormalizations within each bubble in the way described in [25], we obtain to order $1/N$

$$\frac{\delta^2 F}{\delta a_{\mu}^2} \equiv 4\rho_{\parallel, \mu} = \frac{2N}{g_{\mu}} \left(1 + \frac{\gamma_{\mu}}{2N}\right) \left[\left(1 - \frac{g_{\mu}}{\bar{g}_{\mu}^c}\right)^{\nu} + \gamma_{\mu}^{eff} \left(1 + \frac{1}{2N}\right) \left(1 - \frac{g_{\mu}}{\bar{g}_{\mu}^c}\right)^{2\nu} \right]. \quad (3.22)$$

Eqns (3.20) and (3.22) can now be combined to obtain transverse stiffness to order $1/N$

$$4\rho_{\perp, \mu} = \frac{2N}{g_{\mu}} \left(1 + \frac{\gamma_{\mu}}{2N}\right) \left[\left(1 - \frac{g_{\mu}}{\bar{g}_{\mu}^c}\right)^{\nu} - \frac{\gamma_{\mu}^{eff}}{2N} \left(1 - \frac{g_{\mu}}{\bar{g}_{\mu}^c}\right)^{2\nu} \right] \quad (3.23)$$

Finally, using (3.22) and (3.23), we obtain the result for $(\rho_{\parallel, \mu} - \rho_{\perp, \mu})/\rho_{\perp, \mu}$ to order $1/N$. Reexpressing γ_{μ} in terms of correct renormalization group invariants γ_1 and γ_2 of (2.5), and exponentiating logarithmic terms, we obtain the $1/N$ results for the crossover exponents ϕ_1 and ϕ_2 that were given in (2.8). Our value of ϕ_2 coincides with the result by Lang and Ruhl [34] who computed anomalous dimensions of tensor fields of arbitrary rank for critical $O(2N)$ sigma models. On the other hand, there do not seem to be any other computations of ϕ_1 .

B. Uniform susceptibility

The calculation of the uniform susceptibility at small but finite T and arbitrary ρ_\perp is essentially the same as that of $SU(N)$ response at $T \rightarrow 0$; only the summation over frequency should not be substituted by the integration. Doing the same calculations as have let us to (3.20) but at finite T , we obtain to first order in $1/N$

$$\chi_u(T) = \left(\frac{g\mu_B}{\hbar}\right)^2 \bar{\chi}(T) \left(1 + \frac{\gamma_\tau}{2N} \bar{\chi}(T)\right) \quad (3.24)$$

Here

$$\bar{\chi}(T) = \bar{\chi}(T=0) + \delta\bar{\chi}(T) \quad (3.25)$$

where

$$\bar{\chi}(T=0) = \frac{N}{2g_\tau} \left(1 + \frac{\gamma_\tau}{2N}\right) \left(1 - \frac{g_\tau}{\bar{g}_\tau^c}\right)^\nu \quad (3.26)$$

We expect that higher-order corrections to (3.24) will only change γ_τ to γ_τ^{eff} . Notice that at $T \rightarrow 0$, we recover a result consistent with (3.15) and (3.16):

$$\chi_u(T \rightarrow 0) = \left(\frac{g\mu_B}{\hbar}\right)^2 \frac{2}{N} \frac{N\chi_\perp + \chi_\parallel}{(N+1)} \quad (3.27)$$

The temperature dependent piece $\delta\bar{\chi}(T)$ in (3.24) is precisely 1/2 of that in the isotropic $O(2N)$ sigma model with N -dependent spin-wave velocity c^* . At $N = \infty$ we have from [25] $\delta\bar{\chi}(T) = (k_B T / 2\pi c_\perp^2) f(x_1)$, where numerically $f(x_1)$ is close to 1 for all $k_B T / \rho_\perp$. We will describe the structure of $1/N$ corrections to $\delta\bar{\chi}$ and the value of c^* in the following sections: the $1/N$ results are of a rather different physical form depending upon whether $k_B T \gg \rho_\perp$ or $k_B T \ll \rho_\perp$. We will therefore consider the expressions for $\chi_u(T)$ and other observables separately in the renormalized-classical and quantum-critical regions.

We now begin our discussion of various low- T regions.

IV. RENORMALIZED-CLASSICAL REGION

This section will present expressions for different scaling functions in the renormalized-classical region, $k_B T \ll \rho_\perp$. Under this condition, the low-temperature behavior is related to the low-energy fluctuations of the macroscopic order parameter of the ground state and is therefore essentially classical. Indeed, this is true only for fluctuations at sufficiently large scales when typical energies $\hbar\omega \sim \hbar c_\perp k \ll k_B T$, and one need consider only the $\omega_n = 0$ term in the summation over Matsubara frequencies. At larger k , quantum fluctuations are important, and at $k > \xi_J^{-1}$, antiferromagnet possesses $D = 2 + 1$ critical spin fluctuations. We will consider this critical behavior in the next section, and here focus on the situation at small $\hbar c_\perp k < k_B T$. As in unfrustrated antiferromagnets, there are two different low- T regimes already in the classical region, because the actual (thermal) correlation length ξ is exponentially large when $k_B T \ll \rho_\perp$, and one can have either $k\xi \ll 1$ or $k\xi \gg 1$ [35].

Physically, the crossover at $k\xi \sim 1$ is between the regime where the ordering is destroyed by classical fluctuations and the dynamics is purely relaxational ($k\xi < 1$), and the regime where classical fluctuations are weakly damped propagating gapless spin-waves ($k\xi > 1$). Below we will see how the spin structure factor changes in passing from one regime to the other. But first we consider the behavior of the correlation length.

A. Correlation length

As in the collinear case, we define the correlation length from the equal-time, long-distance, $\exp(-r/\xi)$ decay of the spin-spin correlation function. From our previous discussion, especially from (1.11) and (1.12), it is clear that the Fourier transform of the spin correlator is related to the polarization operator rather than to the Green function of the z -field. At $N = \infty$, spinons behave as free particles, and their propagator is $G_0(k, i\omega) = 1/(k^2 + \omega^2 + m_0^2)$, where m_0 is the mass of the z -field, which at $N = \infty$ coincides with the inverse correlation length of the $O(2N)$ model. We then obtain

$$G(\mathbf{r}) \propto \int \frac{e^{i\mathbf{k}\mathbf{r}} d^2k d^2q}{[(\mathbf{q} + \mathbf{k}/2)^2 + m_0^2][(\mathbf{q} - \mathbf{k}/2)^2 + m_0^2]} \propto e^{-2r/m_0} \quad (4.1)$$

We see that in this limit, the actual correlation length, ξ , is precisely $1/2m_0$. We now proceed to finite N . To first order in $1/N$, we have to consider self-energy and vertex corrections within a polarization bubble. A simple inspection of $1/N$ terms shows that while self-energy corrections renormalize the spinor Green function, and hence ξ , vertex corrections only modify the overall factor in the correlation function and do not affect the exponent in the decay rate. In other words, to first order in $1/N$, the actual correlation length is still precisely a half of that for the z -fields, and we therefore only have to locate the pole in the zero-frequency part of the z -field propagator. For the isotropic case ($\gamma_\mu = 0$), such calculations have already been performed in [25]. Here we have to consider also the effect of the γ_μ anisotropy. It is not difficult to check that the anisotropic term contributes to the self-energy to first order in $1/N$, and therefore affects at this order the constraint equation which in essence is the equation for ξ . The γ -dependent self-energy piece can easily be calculated because the only nonvanishing contribution to order $1/N$ comes from the diagram in Fig.1. We obtain

$$\Sigma_\gamma(k, i\omega) = \frac{\gamma_\tau}{2N} \omega^2 + \frac{\gamma_x}{2N} c_0^2 k^2 \quad (4.2)$$

where $c_0 = c_\perp^0 = \sqrt{\rho_\perp^0/\chi_\perp^0}$. Let us first keep only anisotropic self-energy term. Substituting (4.2) into the constraint equation (1.6) and performing the momentum and frequency summation, we obtain

$$\frac{k_B T}{2\pi} \log \frac{k_B T}{\hbar c m} = \frac{1}{g_x} \left(1 - \frac{g_x}{\bar{g}_c}\right) \left(1 + \frac{\gamma_x}{2N}\right), \quad (4.3)$$

where m is the full mass for the z -field, c is the linear combination of the two spin-wave velocities which we will compute below, and \bar{g}_c is the same as in (3.20). We now observe that

the r.h.s. of (4.3) can in fact be reexpressed in terms of the fully renormalized transverse and longitudinal spin-stiffness. Using (3.20) and (3.23), we find

$$\frac{k_B T}{2\pi} \log \frac{k_B T}{\hbar c m} = \frac{2\rho_\perp}{N} \left(1 + \frac{1}{2(N+1)} \frac{(\rho_\parallel - \rho_\perp)}{\rho_\perp} \right) \quad (4.4)$$

Our next step is to determine how (4.4) is modified by other $1/N$ corrections. We first consider the change in the r.h.s. of (4.4) as $T \rightarrow 0$. At $\gamma_\mu = 0$, earlier calculations to order $1/N^2$ [25] have shown that the only temperature-independent modification of the constraint equation is the renormalization of the coupling constant g_x in (4.3) to $g_x (N-1)/N$. This renormalization can effectively be regarded as the wavefunction renormalization of the z -field, such that each z -field propagator acquires a factor $Z = (N-1)/N$. Physically, this renormalization is related to the fact that the solution of the constraint equation at arbitrary small T and finite ρ exists only for $N > 1$, while for $N = 1$ (i.e., for the XY case), a single gapless spin-wave mode has no partner to interact with. Consider now the γ -dependent piece in the r.h.s. of (4.4). Clearly, it should also acquire an extra factor similar to the renormalization of g_x . It is difficult however to determine explicitly the $1/N$ renormalization of the anisotropic term because the anisotropic vertex itself has a factor of $1/N$. On the other hand, the form of the wavefunction renormalization seems quite plausible from a physical perspective, and we assume below, without proof, that it remains the same in the anisotropic case as well. Simple considerations then show that γ_x should be substituted by $\gamma_x/Z = \gamma_x N/(N-1)$. We then obtain, keeping only temperature-independent corrections in the r.h.s. of (4.4)

$$\frac{k_B T}{2\pi} \log \frac{k_B T}{\hbar c m} = \frac{2\rho_s}{N-1} \quad (4.5)$$

where $c^2 = \rho_s/\chi$, and ρ_s and χ are given by

$$\begin{aligned} \rho_s &= \rho_\perp \left(1 + \frac{N}{2(N^2-1)} \frac{(\rho_\parallel - \rho_\perp)}{\rho_\perp} \right) \\ \chi &= \chi_\perp \left(1 + \frac{N}{2(N^2-1)} \frac{(\chi_\parallel - \chi_\perp)}{\chi_\perp} \right) \end{aligned} \quad (4.6)$$

Finally, we collect all temperature-dependent $1/N$ corrections to (4.4) using the same procedure as for the $O(2N)$ model [25]. These corrections include double logarithms in the form $k_B T \log \log k_B T/m$, and regular $O(k_B T)$ terms. Double-logarithms eventually give rise to the temperature-dependent prefactor in ξ . Assembling all contributions, we finally obtain for the actual correlation length in frustrated antiferromagnet

$$\xi = \frac{1}{2} \bar{\xi} \frac{\hbar c}{k_B T} \left(\frac{(N-1)k_B T}{4\pi\rho_s} \right)^{1/2(N-1)} \exp \left[\frac{4\pi\rho_s}{(N-1)k_B T} \right] \quad (4.7)$$

where [36]

$$\bar{\xi} = \left(\frac{e}{8} \right)^{1/2(N-1)} \times \Gamma(1 + 1/2(N-1)) \quad (4.8)$$

We see therefore that, to first order in γ , the expression for the correlation length is the same, up to a factor of $1/2$, as in the $O(2N)$ isotropic sigma-model with effective spin-stiffness $4\rho_s$ and spin-wave velocity c . The factor of 4 in ρ_s merely reflects the difference between the definitions of the coupling constant g in (2.1) and in the $O(2N)$ σ -model. At the same time, the overall factor of $1/2$ is a signature of deconfined spinons. For the physical case of $N = 2$ we have

$$\rho_s = \frac{2}{3}\rho_\perp + \frac{1}{3}\rho_\parallel \quad \chi = \frac{2}{3}\chi_\perp + \frac{1}{3}\chi_\parallel \quad (4.9)$$

To first order in γ we also have $c = 2c_\perp/3 + c_\parallel/3$. The T dependence in (4.7) then agrees with the two-loop renormalization group calculation of ξ performed by Azaria et al [18]. They also obtained the two-loop expression for the correlation length in a classical model, valid at arbitrary ratio of the two bare stiffnesses, and argued that the result for the quantum case at arbitrary γ_μ will be the same if expressed in terms of the fully renormalized ρ_\perp and ρ_\parallel . Our analysis shows that this universal behavior of the correlation length certainly exists to first order in γ_μ , but we have no proof that the universality persists at arbitrary γ_μ . In any event, the analysis presented here is valid close to the critical point when higher order corrections due to anisotropy are small.

B. Uniform susceptibility

The result for $\chi_u(T)$ valid at arbitrary ratio of T/ρ_\perp is given by (3.24). We now use the results of Ref [25] and obtain

$$\delta\bar{\chi}(T) = \frac{N-1}{N} \frac{k_B T}{2\pi c^2} \quad (4.10)$$

where c is given by (4.6). We expect that this result will hold at arbitrary N . For the physical case of $N = 2$ we then obtain using (4.10) and (3.24-3.26)

$$\chi_u = \left(\frac{g\mu_B}{\hbar}\right)^2 \left(\frac{\chi}{\chi_\perp}\right) \left[\chi_\perp + \frac{k_B T}{4\pi c^2}\right] \quad (4.11)$$

In Sec VII we will apply our result for $\chi_u(T)$ to the $S = 1/2$ Heisenberg antiferromagnet on a triangular lattice.

C. Staggered susceptibility and structure factor

The key input for this subsection is our observation, in Eqns. (1.7), (1.12), that the hydrodynamic order-parameter variable for frustrated antiferromagnets is a composite operator made of two z -fields, and spin-spin correlation function is related to the polarization operator of spinons. At $N = \infty$, we use (1.11) and the results of Appendix C, and express $\chi_s(k, i\omega)$ as

$$\chi_s(k, i\omega) = \frac{N_0^2}{4\rho_\perp^2} \Pi(k, i\omega) \quad (4.12)$$

Here N_0 and ρ_\perp are the fully renormalized values of the on-site magnetization and spin-stiffness at $T = 0$, and Π is the polarization operator which for $\hbar ck$, $\hbar\omega \leq k_B T$ is given by [25]

$$\Pi(k, i\omega) = \frac{k_B T}{\pi} \frac{\log \left[\left(k^2 + \tilde{\omega}^2 + \sqrt{(k^2 + \tilde{\omega}^2)^2 + 4k^2 m_0^2} \right) / 2km_0 \right]}{\sqrt{(k^2 + \tilde{\omega}^2)^2 + 4k^2 m_0^2}} \quad (4.13)$$

As before, m_0 is the mass of the z -field at $N = \infty$ which to this order is also the inverse correlation length for the z -field, and $\tilde{\omega} = \omega/c_0$. We see that at small $k \leq m_0$, $\Pi(k, i\omega) \sim k_B T / 4\pi m_0^2$ and hence $\chi_s(k, i\omega) \propto T\xi^2$, where ξ is the actual correlation length. At the same time, at $k\xi \gg 1$, the logarithm in the numerator of (4.13) cancels the overall factor of T , and we obtain $\chi_s(k, i\omega) \propto 1/k^2$ as it should be in the Goldstone regime.

We now consider how this simple behavior is modified by $1/N$ corrections. A simple inspection of the $1/N$ terms shows that the diagrams which contribute to the renormalization of χ_s are the same as in Sec IV A - they include isotropic self-energy and vertex corrections within a polarization bubble, and also corrections due to the γ_μ . Let us first consider the isotropic case. The self-energy corrections to the z -field at $\gamma_\mu = 0$ were studied in [25]. They give rise to a renormalization of the mass and of the bare stiffness, and also yield an overall thermal renormalization factor λ_k for each Green function. For $k \sim \omega/c_\perp \gg m$, this renormalization factor is

$$\lambda_k = \left(\frac{N-1}{N} \right)^{1/2} \left[\frac{\log[k_B T / (\hbar c_\perp m)]}{\log[\sqrt{k^2 + m^2}/m]} \right]^{-1/2(N-1)} \quad (4.14)$$

At $k \sim m$, the logarithm in the denominator is a number of the order of one, and we have $\lambda_k = [k_B T (N-1) / 4\pi \rho_\perp]^{1/2(N-1)} (1 + \mathcal{O}(1/N))$. Further, it is not difficult to check that the vertex renormalization within a bubble also gives rise to logarithmic terms. Evaluating the corresponding diagram in Fig. 3, to accuracy $\mathcal{O}(1)$ and exponentiating the result, we obtain another renormalization factor ζ_k , which at $k \gg m$ and to order $1/N$ is simply $\zeta_k = \lambda_k^2$. Collecting both contributions, we then obtain

$$\chi_s(k, i\omega) = \frac{N_0^2}{4\rho_\perp^2} \lambda_k^4 \Pi(k, i\omega) \quad (4.15)$$

Finally, we consider the effect of the anisotropic term to first order in $1/N$. Clearly, there are self-energy corrections to the z -field propagators which eventually change ρ_\perp to ρ_s and c_\perp to c . Besides, the anisotropic terms give rise to vertex corrections. We didn't perform actual calculations of the vertex corrections, but on general grounds it is likely that, to order $\mathcal{O}(1/N)$, they can be absorbed into the renormalization of N_0 . We then assemble (4.5), (4.13), (4.14) and (4.15) and obtain

$$\chi_s(k, i\omega) = \frac{N_0^2}{\rho_s(N-1)} \left[\frac{k_B T (N-1)}{4\pi \rho_s} \right]^{(N+1)/(N-1)} \xi^2 f(k\xi, \omega\xi/c) \quad (4.16)$$

where the overall factor is chosen such that $f(0, 0) = 1$. It follows from (4.16) that at finite N , $\chi_s(0, 0) \propto \xi^2 T^{(N+1)/(N-1)}$. This result is likely to be valid at arbitrary N . For the

physical case of $N = 2$, it reduces to $\chi_s^{aa}(0, 0) \propto T^3 \xi^2$ - this is substantially smaller than the naive mean-field result $\chi_s(0, 0) \propto T \xi^2$.

The behavior of $f(x, y)$ at intermediate $x, y = O(1)$ is rather complicated, chiefly because the spin-wave velocity also acquires a substantial downturn renormalization at $k\xi = O(1)$ [35]. However at $k\xi \sim \omega\xi/c \gg 1$, the velocity renormalization is irrelevant and using (4.14) and (4.15) we obtain

$$f(x, y) = \left(\frac{N-1}{N+1} \right) \frac{1}{x^2 + y^2} \left(\frac{1}{2} \log(x^2 + y^2) \right)^{(N+1)/(N-1)} \quad (4.17)$$

Substituting this result into (4.16), and using the fact that at $k\xi \gg 1$, $\log x \approx \log \xi$, we obtain to first order in $1/N$

$$\chi_s(k, i\omega) = \left(\frac{2}{N+1} \right) \frac{N_0^2}{2\rho_s} \frac{1}{k^2 + \omega^2/c^2} \quad (4.18)$$

We now demonstrate that at any N , this expression is nothing but the rotationally-averaged spin-wave result for the ordered $SU(N) \times U(1)$ antiferromagnet. Indeed, using (1.11), (1.12) and (3.8) we find that the total number of transverse spin waves in the ordered state is $N_{sw} = 2N$. That (4.18) is the averaged spin-wave result now follows from (1.11) and the fact that each transverse spin-wave mode at $T = 0$ contributes a spin-wave factor $N_0^2/2\rho_s(k^2 + \omega^2/c^2)$ to χ_s (see Appendix C). For the physical case of $N = 2$, the averaging factor is $N_{sw}/N(N+1) = 2/3$, as it should be.

For experimental comparisons, it is also useful to have an expression for the dynamical structure factor $S(k, \omega)$ defined in (1.15), and static structure factor

$$S(k) = \int \frac{d\omega}{2\pi} S(k, \omega) \quad (4.19)$$

As before, we will be interested in the behavior of $S(k, \omega)$ at scales much larger than the Josephson correlation length. At such k , quantum fluctuations are irrelevant, and using (1.16) and (1.26), we can conveniently reexpress $S(k, \omega)$ as

$$S(k, \omega) = \frac{N_0^2}{2\rho_s} \frac{k_B T}{\rho_s} \frac{2\hbar}{1 - e^{-\hbar\omega/(k_B T)}} \bar{\Xi}_1(k, \omega) \quad (4.20)$$

where $\bar{\Xi}_1$ is related in a straightforward manner to the universal function Ξ_1 introduced earlier in (1.26). Below, we will restrict consideration of $\bar{\Xi}(k, \omega)$ to the frequency range $\omega \sim c/\xi$, which is relevant for experimental comparisons in the renormalized classical region.

Consider first, the asymptotic behavior of $\bar{\Xi}(k, \omega)$ at large momentum $k\xi \gg 1$. For such k , we found above that $1/N$ corrections to the polarization operator are not singular. For a qualitative analysis, we can then safely restrict ourselves to $N = \infty$, when the imaginary part of the polarization operator is given by [25]

$$\begin{aligned} \text{Im}\Pi(k, \omega) = & \frac{(\hbar c)^4}{4\pi} \int \frac{d^2q}{4\epsilon_{q_1}\epsilon_{q_2}} [(1 + n_{q_1} + n_{q_2}) (\delta(\epsilon_{q_1} + \epsilon_{q_2} - \hbar\omega) - (\delta(\epsilon_{q_1} + \epsilon_{q_2} + \hbar\omega)) + \\ & (n_{q_1} - n_{q_2}) (\delta(\epsilon_{q_2} - \epsilon_{q_1} - \hbar\omega) - \delta(\epsilon_{q_2} - \epsilon_{q_1} + \hbar\omega))] \end{aligned} \quad (4.21)$$

Here n_q is a Bose function and $\epsilon_q = (\hbar c)\sqrt{q^2 + \xi^{-2}}$. At $ck \gg \omega$, the only contribution to $\text{Im } \Pi(k, \omega)$ comes from the second piece in (4.21), which describes collisionless Landau damping. Doing the integration, we obtain a simple result

$$\bar{\Xi}_1(k, \omega) = \frac{\omega}{2\pi ck^3}. \quad (4.22)$$

Note that as expected, $\bar{\Xi}_1(k, \omega)$ scales linearly with ω .

We turn now to a discussion of smaller k . The corrections to (4.21) include the terms similar to λ_k, ζ_k above, which grow logarithmically with decreasing k and eventually change the temperature dependence of $\bar{\Xi}_1$ at $k\xi \sim 1$. Moreover, at such momenta, the damping of excitations becomes comparable to the real part of the quasiparticle energy, and we cannot simply restrict ourselves to collisionless Landau damping. We did not perform explicit $1/N$ calculations of $\bar{\Xi}_1$ at intermediate k , but for an estimate we can rely on the results of Ref [37,25] for the momentum dependence of the damping of excitations in the $O(2N)$ sigma-model. Combining these results with the expressions (4.16, 4.17) for the real part of χ_s , we obtain

$$\bar{\Xi}_1(k, \omega) \propto \frac{\hbar\omega \gamma_{k\omega}}{\hbar(c_k k^2)^2} \left(\frac{\rho_s^k}{\rho_s} \right)^{2/(N-1)} \quad (4.23)$$

Here $\gamma_{k\omega}$ is the damping of z -field excitations given by [37,25] $\gamma_{k\omega} \propto \hbar c_k k (k_B T / \rho_s^k)^2 \log \rho_s^k / k_B T$, and the momentum-dependent spin-stiffness and spin-wave velocity are introduced as another way to account for the logarithmical terms in (4.17):

$$\rho_s^k = \frac{(N-1)k_B T}{4\pi} \log k\xi; \quad (c_k)^2 \propto \rho_s^k \quad (4.24)$$

(We note in passing that at $k\xi \gg 1$, we have with the logarithmical accuracy $\rho_s^k = \rho_s, c_k = c$.) At $k\xi = \mathcal{O}(1)$, we have $\rho_s^k \propto T, c_k \propto \sqrt{T}$ at *arbitrary* N , and hence, our final result

$$\bar{\Xi}_1(k, \omega) \propto \frac{\omega \xi^3}{c} \left(\frac{(N-1)k_B T}{4\pi \rho_s} \right)^{(5-N)/2(N-1)} \quad (4.25)$$

For $N = 2$, we have $\bar{\Xi}_1(k, \omega) \propto \omega T^{3/2}$.

Finally, we consider the static structure factor, $S(k)$. A simple inspection shows that the frequency integral in (4.19) has two basic contributions. One comes from large ω where the system is $D = 2 + 1$ critical, while the second comes from $\hbar\omega < k_B T$ where the fluctuations are essentially classical. We will see in the next section that at large ω , $\Pi(k, \omega)$ behaves as $1/\omega^{2-\bar{\eta}}$ where $\bar{\eta}$ is given by (2.4). We found earlier that $\bar{\eta} > 1$ (at least, at large N , and hence the frequency integral over quantum fluctuations explicitly depends on the upper cutoff in the theory. We will discuss nonuniversality in $S(k)$ in more detail in the next section. In the renormalized-classical region however, the correlation length is exponentially large and we may expect that the dominant contribution to $S(k)$, which scales as ξ^2 , still comes from the frequencies $\omega \propto \xi^{-1}$ where fluctuations are essentially classical. For such frequencies, the rescaling factor between $\text{Im } \chi(k, \omega)$ and $S(k, \omega)$ is $2/(1 - e^{\hbar\omega/k_B T}) \approx 2k_B T / \hbar\omega$, and we have simply $S(k) = k_B T \chi_s(k, 0)$, where $\chi_s(k, 0)$ is given by (4.16). At $k = 0$ we then obtain $S(0) \propto T^{2N/(N-1)} \xi^2$. For $N = 2$, this reduces to $S(0) \propto T^4 \xi^2$.

D. Local susceptibility and spin-lattice relaxation rate

Another experimentally measured quantity is the momentum-integrated dynamical structure factor $S(\omega) = \int d^2k S(k, \omega)/4\pi^2$. Unlike $S(k)$, this observable is universal in 2D as can easily be seen from (4.22). It is also not difficult to show that for $\omega \sim c\xi^{-1}$, the integration over momentum is confined to $k \sim \xi^{-1}$, where we can use the estimate (4.20, 4.25) for $S(k, \omega)$. We then obtain

$$S_L(\omega) \propto \frac{N_0^2 \xi}{c} \left(\frac{(N-1)k_B T}{4\pi\rho_s} \right)^{(3N+1)/2(N-1)} \quad (4.26)$$

Further, the $\omega \rightarrow 0$ limits of $S(k, \omega)$ and $\chi(k, \omega)$ are related to the transverse ($1/T_1$) and longitudinal ($1/T_2$) relaxation rates for nuclear spins coupled to electronic spins in the antiferromagnet. We have

$$\frac{1}{T_1} = 2 \lim_{\omega \rightarrow 0} \int \frac{d^2k}{4\pi^2 \hbar^2} A_k^2 S(k, \omega) \quad (4.27)$$

$$\left(\frac{1}{T_2} \right)_{NMR}^2 = 2 \lim_{\omega \rightarrow 0} \left(\frac{\rho_s}{\hbar c} \right)^2 \int \frac{d^2k}{4\pi^2 \hbar^2} \bar{A}_k^4 \chi_s^2(k, \omega) \quad (4.28)$$

where A_k and \bar{A}_k are the hyperfine coupling constants (with the dimension of energy). They generally tend to some finite values as $k \rightarrow 0$. The factors of 2 appear because fluctuation modes near Q and $-Q$ equally contribute to relaxation rates. The temperature dependence of $1/T_1$ then immediately follows from the result (4.26) for $S(\omega)$. For $N = 2$ we obtain

$$\frac{1}{T_1} \propto \left(\frac{A_0}{\hbar} \right)^2 \frac{N_0^2 \xi}{c} \left(\frac{k_B T}{\rho_s} \right)^{7/2} \quad (4.29)$$

An exactly parallel computation can be done for the spin-echo decay rate $1/T_2$, and the result is (for general N)

$$\frac{1}{T_2} \propto \left(\frac{\bar{A}_0}{\hbar} \right)^2 \frac{N_0^2 \xi}{\hbar^2 c} \left(\frac{k_B T}{\rho_s} \right)^{(N+1)/(N-1)} \quad (4.30)$$

For $N = 2$ this yields $T_2^{-1} \propto T^3 \xi$.

V. QUANTUM-CRITICAL REGION

We now consider the results for the quantum-critical region where $4\pi\rho_s < Nk_B T$. Under this condition, the relevant scale for fluctuations is given by T itself and both quantum and classical fluctuations are equally important (i.e., at relevant energies, Bose functions are $O(1)$). Our first observation in this region concerns the role of the anisotropic (i.e. γ_μ dependent) terms in the action. The scaling hypothesis predicts that any scaling function near the quantum transition should depend on the dimensionless ratio ξ_J/L_τ where ξ_J is the Josephson correlation length, and $L_\tau = \hbar c/k_B T$ is a finite length in the imaginary

time direction at $g = g_c$. We have shown above in Sec III that at $T = 0$, anisotropic corrections had a form $\gamma_\mu(\xi_J/a)^{-\phi_{1,2}}$ where both crossover exponents are clearly positive and even larger than 1 at finite N (see Eqn. (2.8)). We therefore expect that the leading anisotropic corrections deep in the quantum-critical region will scale as $\gamma_\mu(k_B T a/\hbar c)^{\phi_{1,2}}$ with positive $\phi_{1,2}$, i.e. they will be subdominant at low T compared to the leading terms in the scaling functions. Clearly then, the quantum-critical behavior will be the same as in the isotropic $O(2N)$ sigma-model. The anisotropic term in the action will however renormalize the spin-wave stiffnesses and velocities in the subleading terms in the full scaling functions, which describe deviations from the pure critical behavior. These terms will be calculated in this Section only at $N = \infty$, at which order the anisotropic term in the action does not contribute. We will then assume, without proof, that the renormalization due to γ_μ leads to the same effective ρ_s and χ given by (4.6) as the renormalized-classical expressions. On general grounds, this is likely to be the case because the corrections to the pure quantum-critical formulas account for the crossover to the renormalized-classical region. However, as we said, explicit calculation of the subleading terms at finite N has not been performed.

We emphasize that even in the absence of the anisotropy, the scaling properties of spin correlators are quite different from those for unfrustrated antiferromagnets simply because each spin component is a bilinear product of the z -fields. We now consider separately the behavior of various observables.

A. Correlation length

The expression for the correlation length follows directly from the observation that the spin propagator is a convolution of two Green functions for z -fields. An analysis, similar to that for the renormalized-classical region, shows that vertex corrections in the polarization bubble do not effect the form of the exponential decay of correlations, and therefore the actual correlation length is again exactly 1/2 of that for the $O(2N)$ sigma-model. Specifically, we obtain

$$\xi(T) = \frac{1}{2} \frac{\hbar c}{k_B T} X_1(\infty) \left[1 - \kappa \bar{x}_1^{-1/\nu} + \dots \right] \quad (5.1)$$

where we defined $\bar{x}_1 = N k_B T / 4\pi \rho_s$, and ν is the exponent for the Josephson correlation length given by (2.4). The values of $X_1(\infty)$ and κ were found earlier [25]: $X_1(\infty) = \Theta(1 + 0.1187/N)$, where $\Theta = 2 \log(1 + \sqrt{5})/2 = 0.962424$, and $\kappa = 2/\sqrt{5} + O(1/N)$.

B. Uniform susceptibility

We continue with the response to the uniform magnetic field. As in the renormalized-classical region, we use the general result (3.24), but now the temperature dependent piece in $\bar{\chi}$ is dominant, and to order $1/N$ the universal function for χ_u defined in (1.35) is given by

$$\Omega(x_1, y_\rho, y_\chi) = \frac{\sqrt{5}}{2\pi} \log \frac{\sqrt{5} + 1}{2} \left[\left(1 - \frac{0.31}{N} \right) + \alpha \bar{x}_1^{-1/\nu} + \dots \right] \quad (5.2)$$

where $\alpha = 0.8 + O(1/N)$. This is indeed a half of the susceptibility for $O(2N)$ square-lattice antiferromagnet. At $N = 2$, we obtain using the mean-field ($N = \infty$) result for the correction term

$$\chi_u(T) = \left(\frac{g\mu_B}{\hbar}\right)^2 \left[0.86\chi + 0.145\frac{k_B T}{c^2}\right] \quad (5.3)$$

C. Dynamic susceptibility and structure factor

In this subsection, we compute the scaling functions $\Phi_{1s}(\bar{k}, \bar{\omega}, x = \infty, y_\rho = 0, y_\chi = 0) = \Phi_s(\bar{k}, \bar{\omega})$ and $\Xi_1(\bar{k}, \bar{\omega}, x = \infty, y_\rho = 0, y_\chi = 0) = \Xi(\bar{k}, \bar{\omega})$ for staggered dynamical susceptibility and structure factor at the critical point $g = g_c$. These two scaling functions were introduced in (1.26) and are related by the fluctuation-dissipation theorem $\Xi(\bar{k}, \bar{\omega}) = \text{Im}\Phi_s(\bar{k}, \bar{\omega})$. As before, $\Phi_s(\bar{k}, \bar{\omega})$ is simply related to the polarization operator for $z-$ fields: $\Phi_s(\bar{k}, \bar{\omega}) = (k_B T / 2(\hbar c_\perp)^2) \Pi(k, \omega)$. The limiting behavior of Π and hence $\Phi_s(\bar{k}, \bar{\omega})$ at small and large \bar{k} and $\bar{\omega}$ can be obtained by properly expanding the real part of (4.13). For large $\bar{k}, \bar{\omega}$, we found using the results of [25,38]

$$\Phi_s(\bar{k}, \bar{\omega}) = \frac{1}{16\sqrt{\bar{q}^2 - (\bar{\omega} + i\delta)^2}} + \frac{8\zeta(3)}{5\pi} \frac{2(\bar{\omega}^2 + \bar{q}^2)}{(\bar{k}^2 - (\bar{\omega} + i\delta)^2)^3} + O\left(\frac{1}{(\bar{k}, \bar{\omega})^6}\right) \quad (5.4)$$

On the other hand, at small momentum and frequency, an expansion in the real part of (4.13) yields

$$\text{Re } \Phi_s(\bar{k}, \bar{\omega}) = \frac{\sqrt{5}}{16\pi\Theta} \left(1 - \frac{\bar{k}^2(1 + 2\Theta/\sqrt{5}) - \bar{\omega}^2}{12\Theta^2} + O((\bar{k}, \bar{\omega})^4)\right) \quad (5.5)$$

We consider next $1/N$ corrections to these results. At small \bar{k} and $\bar{\omega}$, the expansion in $1/N$ does not involve logarithms. Regular $1/N$ corrections to Φ_s were found to be quite small for unfrustrated antiferromagnets [25] and we expect the same to be true in our case as well. On the other hand, at $\bar{k}, \bar{\omega} \gg 1$, the behavior is nearly the same as at the critical point at $T = 0$, and using the results of Appendix C we found that the leading term in (5.4) is modified to

$$\Phi_s(\bar{k}, \bar{\omega}) = \frac{A_N}{16(\bar{q}^2 - (\omega + i\delta)^2)^{1-\bar{\eta}/2}} \quad (5.6)$$

where $A_N = 1 + O(1/N)$ and $\bar{\eta}$ is given by (2.4)

It is also not difficult to compute explicitly the imaginary part of the polarization operator, which then yields the scaling function for the dynamic structure factor. In the two asymptotic limits of large and small $\bar{\omega}$ we obtained

$$\Xi(\bar{k}, \bar{\omega}) = \frac{A_N \sin(\pi\bar{\eta}/2)}{16} \frac{\theta(\bar{\omega}^2 - \bar{k}^2)}{(\bar{\omega}^2 - \bar{k}^2)^{1-\bar{\eta}/2}} \quad (5.7)$$

for $\bar{\omega} \gg 1$ and

$$\Xi(\bar{k}, \bar{\omega}) = \frac{\bar{\omega}}{8\sqrt{\pi}} \frac{\exp -\bar{k}/2}{\bar{k}^{3/2}} \quad (5.8)$$

for $\bar{\omega} \ll 1$ and $\bar{k} \gg 1$. In (5.7), $\theta(x)$ is a step function. It is also not difficult to obtain the $N = \infty$ expression for Ξ for both $\bar{\omega} \ll 1$ and $\bar{k} \ll 1$, but in this region of momentum and frequency, quasiparticle excitations are overdamped, and one again cannot restrict to the $N = \infty$ result of collisionless Landau damping. We can only expect on general grounds that at small $\bar{\omega}$ and arbitrary \bar{k} , $\Xi(\bar{k}, \bar{\omega}) \propto \bar{\omega}$.

We consider, further, the static structure factor $S(k)$ defined by (4.19). In the quantum-critical region, we have at $g \nearrow g_c$

$$S(\bar{k}) = \frac{N_0^2}{2} \left(\frac{\hbar c}{\rho_s} \right)^2 \left(\frac{Nk_B T}{4\pi\rho_s} \right)^{\bar{\eta}-1} I(\bar{k}) \quad (5.9)$$

where $I(\bar{k}) = \int d\bar{\omega} (1 - e^{-\bar{\omega}})^{-1} \Xi(\bar{k}, \bar{\omega})/\pi$. Notice that the functional form of $S(\bar{k})$ is similar to that for unfrustrated antiferromagnets [25]. Moreover, in both frustrated and unfrustrated cases, $\Xi(\bar{k}, \bar{\omega}, \infty)$ behaves at large frequencies as $\Xi(\bar{k}, \bar{\omega}, \infty) \propto (\bar{\omega})^{-2+\bar{\eta}}$. The difference between the two cases is in the value of $\bar{\eta}$. For unfrustrated antiferromagnets, $\bar{\eta} \approx 0$ and the frequency integral in $I(\bar{k})$ is convergent. For frustrated systems, $\bar{\eta} > 1$ at least, at large N (see (2.4)), and the integral over frequency in $I(\bar{k})$ is divergent, which actually means that the dominant contribution to $S(\bar{k})$ at small temperatures comes from the frequencies of the order of a cutoff. Specifically, using (4.13) we obtain

$$I(\bar{k}) = \frac{B_N}{\bar{\eta} - 1} \left[\left(\bar{\Lambda}^{\bar{\eta}-1} - \Theta^{\bar{\eta}-1} \right) \right] + I'(\bar{k}) \quad (5.10)$$

Here $B_N = 1 + \mathcal{O}(1/N)$, Θ was defined after (5.1), $\bar{\Lambda} = \hbar c \Lambda / k_B T$ where Λ is a relativistic cutoff in the theory, and $I'(\bar{k})$ is a universal function of momentum, which as $\bar{k} \rightarrow 0$ tends to $I'(0) = 1.67 + \mathcal{O}(1/N)$. The nonuniversality in $I(\bar{k})$ at low temperatures is now transparent. Recall however that (5.10) is valid only in the quantum-critical regime where the temperature is the only scale for fluctuations. In the renormalized-classical regime, the analog of $I'(\bar{k})$ is proportional to the square of the actual correlation length ξ , and is exponentially large at low T compared to the nonuniversal piece in $I(\bar{k})$, which does not contain any dependence on ξ .

D. Local susceptibility and spin-lattice relaxation

Unlike $S(\bar{k})$, the momentum-integrated dynamic structure factor $S_L(\omega) = \int d^2k S(k, \omega)/4\pi^2$ is universal in $2d$, as we already found in the renormalized-classical region. The scaling function for $S_L(\omega)$ was introduced in (1.36). At $g = g_c$ and $N = \infty$, this scaling function can be deduced directly from (4.13). A simple calculation yields

$$K(\bar{\omega}) = \frac{1}{32\pi} \left[2 \log \frac{1 - e^{-(\Theta+\bar{\omega})}}{1 - e^{-\Theta}} + \Theta(\bar{\omega} - 2\Theta) \left(\bar{\omega} - 2\Theta + 2 \log \frac{1 - e^{-(\bar{\omega}-\Theta)}}{1 - e^{-\Theta}} \right) \right] \quad (5.11)$$

where $K(\bar{\omega}) = K_1(\bar{\omega}, x_1 = \infty, y_\rho = 0, y_\chi = 0)$. At small $\bar{\omega}$, this reduces to

$$K(\bar{\omega}) = \frac{\sqrt{5} - 1}{64\pi} \bar{\omega} \quad (5.12)$$

while at $\bar{\omega} \gg 1$, we have

$$K(\bar{\omega}) = \frac{\bar{\omega}}{32\pi} \quad (5.13)$$

Note that linear dependence on $\bar{\omega}$ is present in both limits (in the unfrustrated case, $K(\bar{\omega})$ saturated at large $\bar{\omega}$).

We now consider $1/N$ corrections to these results. At $\bar{\omega} \ll 1$, the expansion in $1/N$ is free from divergences because each z - field propagator has a gap $\Theta \sim 1$. The expansion in $1/N$ then holds in integer powers of $1/N$, and numerically we expect the corrections to (5.12) to be quite small. On the contrary, at large $\bar{\omega} \gg 1$, the actual form of $K(\bar{\omega})$ is different from the $N = \infty$ result because of the singular $1/N$ corrections. Using (5.7) we obtain instead of (5.13)

$$K(\bar{\omega}) = \frac{A_N \sin(\pi\bar{\eta}/2) \bar{\omega}^{\bar{\eta}}}{32\pi \bar{\eta}} \quad (5.14)$$

Finally, the $\bar{\omega} \rightarrow 0$ limit of $S_L(\bar{\omega})$ is related to the transverse spin-lattice relaxation rate. As before, we assume that the hyperfine coupling constant A_k tends to a finite value at $k = 0$ and the dominant contribution to $1/T_1$ thus comes from the momentum range $\bar{k} = O(1)$. Using (1.36), (4.28) and (5.12), we then obtain

$$\frac{1}{T_1} = \left(\frac{A_0}{\hbar}\right)^2 Z \frac{N_0^2 \hbar}{\rho_s} \left(\frac{Nk_B T}{4\pi\rho_s}\right)^{\bar{\eta}} \quad (5.15)$$

where $Z = (\sqrt{5} - 1)/8N + O(1/N^2)$.

A parallel analysis can be done for longitudinal spin-lattice relaxation $1/T_2$ defined in (4.28), and the result is

$$\frac{1}{T_2} \propto \left(\frac{\bar{A}_0}{\hbar}\right)^2 \frac{N_0^2 \hbar}{\rho_s} \left(\frac{Nk_B T}{4\pi\rho_s}\right)^{\bar{\eta}-1} \quad (5.16)$$

VI. QUANTUM DISORDERED REGION

Let us first notice some crucial properties of the quantum-disordered ($g > g_c$) phase at $T = 0$. The presence of free spin-1/2 z quanta implies that $\chi_s(k, \omega)$ only has a branch cut in the complex ω plane. This should be contrasted with the behavior of collinear antiferromagnets [25] which had an additional spin-1 quasiparticle pole. We will compute below the structure of this branch cut at $N = \infty$.

Before doing this, it is useful to introduce our precise definition of the prefactor \mathcal{A} . We will use the $T = 0$ form of the local dynamic structure factor $S_L(\omega)$ to specify the

normalization. Using the fact that the dynamic susceptibility involves a response function with 2 spinon intermediate states, each with a gap Δ , and that each spinon propagator has a quasiparticle pole we can show quite generally (to all orders in $1/N$ or $\epsilon = 4 - D$) that near the threshold in the quantum disordered phase we must have

$$S_L(\omega) = \mathcal{A} \frac{\hbar\omega - 2\Delta}{2\Delta} \theta(\hbar\omega - 2\Delta) \quad \omega \text{ close to } 2\Delta. \quad (6.1)$$

The above form *defines* the values of \mathcal{A} and Δ . Combined with c , these parameters universally determine the entire staggered susceptibility.

The $N = \infty$ computation of χ_s is standard [25]. The z propagators acquire a gap Δ given by

$$\Delta = 4\pi \left(\frac{1}{g_c} - \frac{1}{g} \right) \quad (6.2)$$

We evaluated the susceptibility using (1.11) and found at $N = \infty$

$$\text{Im}\chi_s(k, \omega) = \text{sgn}(\omega) \frac{\mathcal{A}\pi c^2}{2\Delta} \frac{1}{\sqrt{\omega^2 - c^2 k^2}} \theta\left(\omega^2 - c^2 k^2 - 4\Delta^2/\hbar^2\right) \quad (6.3)$$

with $\mathcal{A} = g^2\Delta/(4\pi\hbar^2)$. These results are consistent with (1.28) and (1.32) provided $\nu = 1$ and $\bar{\eta} = 1$. Note that $\chi_s(k, \omega)$ has branch cuts emanating from $\pm(4\Delta^2/\hbar^2 + c^2 k^2)$ to $\pm\infty$. Compare this result with the confined spinon model of ([25]) where at $N = \infty$, $\text{Im}\chi_s$ was simply a delta function.

It is simple to extend the above results for χ_s to finite temperature and to order $1/N$. The main effect of small T is to fill in the gap in the spectrum by exponentially small terms. The $1/N$ corrections do not introduce any essentially new features, and will not be considered here.

VII. APPLICATION TO A $S = 1/2$ ANTIFERROMAGNET

In this section, we compare our scaling results to the properties of the $S = 1/2$ Heisenberg antiferromagnet on a triangular lattice. As input, we need the values of sublattice magnetization, two spin stiffnesses and two spin-susceptibilities at $T = 0$. In Appendix B, we have calculated these parameters in the $1/S$ expansion, to order $1/S$ for the stiffnesses and susceptibilities and to order $1/S^2$ for sublattice magnetization. The extension of our large S results to $S = 1/2$ yields

$$N_0 = 0.266; \quad \chi_{\perp} = \frac{0.091}{Ja^2} \quad \chi = \frac{0.084}{Ja^2}, \quad \rho_s = 0.086J, \quad c = \sqrt{\rho_s/\chi} = 1.01Ja \quad (7.1)$$

The magnitude of the $1/S^2$ result for the sublattice magnetization indicates that higher-order corrections are rather small.

Let us now summarize the scaling predictions which follow from the values in (7.1). For the uniform susceptibility, we obtain

$$\chi_u = \left(\frac{g\mu_B}{\hbar a}\right)^2 \frac{1}{J} \left[0.084 + 0.07\frac{k_B T}{J}\right] \quad (7.2)$$

in the renormalized-classical regime, and (using the $N = \infty$ result for the correction term)

$$\chi_u = \left(\frac{g\mu_B}{\hbar a}\right)^2 \frac{1}{J} \left[0.072 + 0.14\frac{k_B T}{J}\right] \quad (7.3)$$

in the quantum-critical regime. Comparing (7.2) and (7.3), we observe that the slope of χ_u in the quantum-critical regime is nearly twice as large as in (7.2), while the value of the intercept is larger in the renormalized-classical regime. Further, the correlation length behaves in the renormalized-classical regime as

$$\xi \approx 0.24 \left(\frac{4\pi\rho_s}{k_B T}\right)^{1/2} \exp[4\pi\rho_s/k_B T] \quad (7.4)$$

where $4\pi\rho_s \approx 1.08J$, and deep in the quantum-critical region as

$$\xi = \frac{0.51Ja}{k_B T} \quad (7.5)$$

Finally, in the renormalized-classical regime, the universal contribution to $S(k)$ is dominant, and for $k = 0$ we obtain from (4.16) and (4.19)

$$S(0) \approx 0.85 \left(\frac{k_B T}{4\pi\rho_s}\right)^4 \xi^2 \quad (7.6)$$

In the quantum-critical region, the dominant piece in $S(0)$ is a temperature-independent contribution from lattice scales, and we can only conclude that deep inside quantum-critical region, $S(0) \sim A + B(T/T_0)^{\bar{\eta}-1}$, where A is a T -independent nonuniversal piece. Using the large N results we found $B \approx -0.27a^2$ and $T_0 \approx 0.54J$.

From the discussion in the bulk of the paper, we expect the crossover between the classical and quantum regimes to occur somewhere around $x_1 = 1$ i.e. at $k_B T = 2\pi\rho_s \sim 0.5J$. This indeed is not a very small crossover temperature. However, the analysis for the unfrustrated case [25] shows that the uniform susceptibility displays quantum-critical behavior starting already below $x_1 = 1$. We therefore first compare our results with the numerical data on uniform susceptibility.

The temperature dependence of χ_u was recently studied in high-temperature series expansions for $S = 1/2$ triangular antiferromagnet [40]. The data show that χ_u obeys a Curie-Weiss law at high T , passes through a maximum at $T \approx 0.4J$, and then falls down. In general, the temperature where χ_u has a maximum roughly separates the low-temperature region below the maximum where a long-wavelength approach is valid, from the high-temperature region where the physics is dominated by lattice-scale effects. It is unfortunate that this temperature is rather low for the triangular antiferromagnet, because it reduces substantially the temperature range for low-energy behavior (for comparison, in the square-lattice antiferromagnet, the maximum in T_c occurs at $k_B T \sim J$). Numerical data [40] is available only over a small T region below the maximum. Nevertheless, we fitted the data by a linear

in T dependence and found 0.13 ± 0.03 for the slope and around 0.06 for the intercept - both results are in reasonable agreement with our quantum-critical expression (7.3). Finally, at very low T , we expect a crossover to the renormalized-classical regime, and the $T = 0$ value in (7.2) is also consistent with the data.

Now about $S(0)$. Previous studies of square-lattice antiferromagnets have shown that we can hardly expect to observe pure quantum-critical behavior for $S(0)$ at $x_1 \sim 1$. Indeed, the leading correction to $S(0)$ due to the deviation from purely quantum-critical behavior is $\delta S(0) = C(2\pi\rho_s/k_B T)$, where at $N = \infty$ we found $C = 0.45a^2$. Clearly then, at $k_B T \sim 0.5J$, temperature dependence related to deviations from pure criticality is likely to overshadow the weak $((T/T_0)^{\bar{\eta}-1})$ temperature dependence in $S(0)$ at $g = g_c$; instead, we expect that at such T , the structure factor should roughly follow $S(0) = A + C(2\pi\rho_s/k_B T)$, or (still considering second term as a correction) $k_B T \log S(0) \approx 2\pi\rho_s C/A + k_B T \log A$. The series expansions [40] yielded $k_B T \log S(0)$ which increases linearly with T upto about $0.5J$. This is consistent with our crossover expression, but inconsistent with the renormalized-classical formula, (7.6) which predicts that $k_B T \log S(0)$ decreases with temperature. We therefore do not believe that the numerical data correspond to the classical regime, as was suggested in Ref [40].

Finally, the correlation length. Series expansions reported that ξ is approximately one lattice spacing at $k_B T = 0.4J$. This is substantially lower than our renormalized-classical result $\xi_{cl} \approx 5a$ at the same temperature, but is consistent with the value of ξ deep in the quantum-critical regime $\xi_{quant} \approx 1.25a$. We emphasize however that Ref. [40] defined ξ as $\xi^2 = -(1/S(k))(\partial S/\partial k^2)|_{k=0}$ - this definition yields a nonuniversal value of ξ for quantum-critical frustrated antiferromagnets. On the contrary, our definition of ξ , from the long-distance decay of spin-spin correlator, always yields a universal result. Besides, even if the universal piece in $S(k)$ is dominant, as in the renormalized classical regime, the two definitions are still nonequivalent even at $N = \infty$ simply because spin structure factor is related to the polarization operator of z -fields, which unlike z -field propagator, does not have a Lorentzian form. In the classical regime, the rescaling factor between the two definitions of ξ is $\xi_{series}^2 = (2/3)\xi_{ours}^2$ at $N = \infty$. The value of the rescaling factor in the intermediate and quantum-critical regimes is difficult to estimate, but on general grounds it should be smaller than $2/3$ because the nonuniversal piece in $S(0)$ becomes dominant at $g = g_c$. We therefore expect that the actual correlation length is in fact larger than reported in [40]. This again is consistent with our observation that at $k_B T$ around $0.4J$, the system is in the crossover region between renormalized-classical and quantum-critical regimes, and is probably closer at $k_B T = 0.4J$ to the quantum-critical regime.

VIII. CONCLUSIONS

In conclusion, we summarize our main results. We have presented a general scaling framework to describe frustrated antiferromagnetic systems near the quantum phase transition between classically ordered and quantum-disordered ground states.

We considered various scaling functions for experimentally measurable quantities both on the ordered and disordered sides of the quantum transition and have shown that the observables which probe the behavior of antiferromagnets at low energies are completely

universal functions of just a few measurable parameters at $T = 0$. On the ordered side, these parameters are sublattice magnetization and transverse and longitudinal spin-stiffness and spin susceptibility.

We then specialized to particular field-theoretic model of the transition (results for a different model are briefly noted in Appendix A) Our approach began with the fundamental assumption that the disordering transition at $T = 0$ is continuous and that vortex-like excitations with a nonzero local Z_2 flux are irrelevant at low energies. We showed that, in this situation, the proper low-energy theory near the transition is given by the $SU(2) \times U(1)$ sigma-model for spinon fields. All physically observable excitations are collective modes of two spinons. The global $SU(2)$ symmetry of the sigma-model action is related to spin rotations, while the global $U(1)$ symmetry is related to lattice transformations [29]. For triangular and other commensurate noncollinear antiferromagnets, this lattice symmetry in fact reduces to a discrete symmetry (Z_3 symmetry in case of triangular antiferromagnets). At the quantum transition point, the symmetry of the action enlarges to $O(4)$.

We then extended our action to a general N by considering spinons as N -component objects, and used the powerful technique of $1/N$ expansion. The extended action has $SU(N) \times U(1)$ symmetry. The fixed point in this approach has its internal symmetry enlarged from $SU(N) \times U(1)$ to $O(2N)$ for *any* N .

We then used the $1/N$ expansion to explicitly compute the scaling properties of the field-theory, always finding that they were consistent with the more general scaling ansatzes. We made definite predictions for the dynamic structure factor, static susceptibility, correlation length, local and static structure factors, and the spin-lattice relaxation rate in the renormalized-classical and quantum-critical regions. We also briefly discussed the low- T behavior in the quantum-disordered region.

Finally, we compared our results to the properties $S = 1/2$ triangular antiferromagnets. We determined the input parameters in the scaling function from a $1/S$ expansion on the original lattice Hamiltonian, and made quantitative predictions about the form of uniform susceptibility, correlation length and static structure factor. We compared the results with the data of recent high-temperature series expansions. All of the data were consistent with the interpretation that there is a narrow window of quantum-critical behavior just below the temperature at which the uniform susceptibility passes through its maximum. However, more detailed numerical and experimental results are needed before any definitive conclusions can be reached. We hope that it will be possible to perform measurements in a T range between the $3d$ ordering temperature and the temperature where uniform susceptibility has a maximum. Our prediction is that in between the two temperatures, the uniform susceptibility should follow our formula for the quantum-critical regime.

IX. ACKNOWLEDGEMENTS

The research was supported by NSF Grant No. DMR-92 24290. We are pleased to thank P. Azaria, B. Delamott, P. Lecheminant, D. Mouhanna, and N. Read for useful discussions and communications

APPENDIX A: FIELD THEORY WITH CONFINED SPINONS

In the event there is continuous transition from the magnetically ordered state to a quantum-disordered state with *confined* spinons, we expect that it can be described by a continuum field theory of the \mathbf{n}_1 and \mathbf{n}_2 fields themselves. All fields are now singlets under the Z_2 gauge symmetry and the Z_2 vortices are permitted. Such large- M field theories have been considered earlier by Kawamura [28] and Azaria *et. al.* [29]. A potential problem with this approach is that the results of the $D = 2 + \epsilon$ analysis [18] are not obviously consistent with the $D = 4 - \epsilon$ and large M theories. The universal properties of such nearly-critical antiferromagnets are rather similar to those of the collinear antiferromagnets considered in Ref. [25]. Therefore we will be rather brief, as the analog of all the results in the body of this paper can be obtained by minor modifications of those of Ref [25].

We will consider the action

$$\mathcal{Z} = \int \mathcal{D}\mathbf{n}_1 \mathcal{D}\mathbf{n}_2 \exp \left[-\frac{1}{2} \int d^D x \left(p_{1,\mu} \left((\partial_\mu \mathbf{n}_1)^2 + (\partial_\mu \mathbf{n}_2)^2 \right) + p_{2,\mu} (\mathbf{n}_1 \partial_\mu \mathbf{n}_2 - \mathbf{n}_2 \partial_\mu \mathbf{n}_1)^2 + V(\mathbf{n}_1, \mathbf{n}_2) \right) \right] \quad (\text{A1})$$

where $p_{1,\mu} = \rho_{\perp,\mu}^0$, $p_{2,\mu} = (\rho_{\parallel,\mu}^0 - 2\rho_{\perp,\mu}^0)/4$. The potential $V(\mathbf{n}_1, \mathbf{n}_2)$ can either impose the hard-spin constraints (in a $D = 2 + \epsilon$ expansion)

$$\mathbf{n}_1^2 = \mathbf{n}_2^2 = 1 \quad ; \quad \mathbf{n}_1 \cdot \mathbf{n}_2 = 0 \quad (\text{A2})$$

or the soft-spin potential (in a $D = 4 - \epsilon$ expansion)

$$V(\mathbf{n}_1, \mathbf{n}_2) = \frac{1}{2} r_0 (\mathbf{n}_1^2 + \mathbf{n}_2^2) + u_1 (\mathbf{n}_1^2 + \mathbf{n}_2^2)^2 + u_2 (\mathbf{n}_1 \times \mathbf{n}_2)^2 \quad (\text{A3})$$

Kawamura [28] introduced a large M expansion of (A1) in which the vectors $\mathbf{n}_1, \mathbf{n}_2$ are generalized to M -components; the action then has a $O(M) \times O(2)$ symmetry. The relationships between the large M , $\epsilon = D - 2$, and $\epsilon = 4 - D$ expansions have been discussed by Azaria *et. al.* [29].

Here we will discuss some simple properties of the large M expansion. The results have striking differences from the large N expansion of this paper, in particular, the phase transition at $M > 3$ belongs to the universality class different from $O(M+1)$ model. Which of these two expansions is more appropriate for the physical case $M = 3, N = 2$ is not quite clear, and numerical studies of frustrated antiferromagnets will be quite useful in this regard. The most obvious difference is of course in the absence of spinons in the large M theory. The staggered susceptibility $\chi_s(k, \omega)$ now has delta-function quasiparticle peaks, in contrast to the branch cuts of the large N theory. Differences also appear in the behavior of the correlators of the conserved charges and currents. A key property of the $1/M$ expansion is that the $p_{2,\mu}$ couplings are irrelevant. This immediately implies that the universal ratios of the stiffnesses (Eqn (1.21)) obey $\Upsilon_\rho = \Upsilon_\chi = 2$ at $M = \infty$. We computed Υ to first order in $1/M$ and obtained

$$\Upsilon_\rho = \Upsilon_\chi = 2 - \frac{26}{3\pi^2 M} \quad (\text{A4})$$

In performing the $1/M$ calculations, we introduced three Lagrange multipliers in the functional integral to impose the constraints (A2), and also introduced condensates of the n_1 and n_2 fields. The computations are a bit tricky: we found that the $1/M$ correction to Υ is related to the difference in the Green functions of the transverse components of $n_{1,2}$ and the fluctuating components along the directions of the condensates. This difference clearly disappears at $g = g_c$; however the correction to the ratio of the stiffnesses (i.e., to $O(k^2)$ in the full Green functions) remains finite at $g = g_c$ because it includes integrals which are divergent at $g \rightarrow g_c$.

Also interesting is the behavior of the uniform susceptibility $\chi_u(T)$ in the quantum-critical region. It is simple to show that at $M = \infty$ this is given by precisely *twice* the mean-field result of Ref [25], with $c \rightarrow c_\perp$. Contrast this with the result of the deconfined spinon model of the body of the paper: there we found that the $N = \infty$ result was *one-half* the result of Ref [25] !

APPENDIX B: SPIN-WAVE CALCULATIONS AT $T = 0$

For experimental comparisons of the results obtained within $1/N$ expansion, we need the $T = 0$ expressions for sublattice magnetization, spin-wave velocities and uniform spin susceptibilities. Below we will calculate these quantities for the Heisenberg antiferromagnet on a triangular lattice in an expansion in $1/2S$, where S is the value of the spin. Though we will use large S approach, our chief interest is in the case of $S = 1/2$ when quantum fluctuations are the strongest. As we will see below, the convergence of the perturbative series in $1/2S$ in triangular antiferromagnets is very good (as it is on the square lattice [43,44]), and the $1/S$ expansion is likely to give quite accurate values of observables, even for $S = 1/2$.

We now turn to a description of the calculations. We consider here the model with interactions between nearest neighbors:

$$\mathcal{H} = J \sum_{\mathbf{l}, \Delta} \mathbf{S}_{\mathbf{l}} \mathbf{S}_{\mathbf{l} + \Delta}. \quad (\text{B1})$$

The procedure of doing the $1/S$ expansion is rather standard and involves several steps which include (i) the transformation from spin operators to bosons via Holstein-Primakoff, Dyson-Maleev, or some other transformation, (ii) the diagonalization of the quadratic form in bosons, and (iii) the use of a standard perturbative technique for Bose-liquids to treat the interaction between spin waves. Noninteracting spin waves have energy which scales as S , while the interaction vertex involving m bosons scales as $S^{2-m/2}$; this gives rise to an expansion in powers of $1/S$ for anharmonic contributions, similar to that in a weakly interacting Bose gas.

Another important issue related to the $1/S$ expansion, is the number of boson fields which one has to introduce in order to keep track of the whole spin-wave spectrum, not just the low-energy modes. This is important because quantum fluctuations are not divergent in $2d$, and the $1/S$ expansion involves sums over the whole Brillouin zone. In the general case, the number of different boson fields is equivalent to the number of magnetic sublattices. However, in several special cases, a multisublattice magnetic configuration can be transformed into a one-sublattice ferromagnetic one by applying a uniform twist on the coordinate frame. In this

situation, the spin-wave spectrum has no gaps at the boundaries of the reduced Brillouin zone and one can describe all excitations by a single bosonic field, as in the case of a ferromagnet. Obviously, the triangular antiferromagnet in a zero magnetic field is an example of such special behavior: the 120° ordering becomes a ferromagnetic one in the twisted coordinate frame with a pitch $Q = (4\pi/3, 4\pi/\sqrt{3})$. We therefore will use a one-sublattice description of triangular antiferromagnet whenever possible. This indeed substantially simplifies the calculations.

We start with the transformation from spin operators to bosons. The choice of the transformation is indeed only a matter of convenience, and the final results are independent of the way how bosons are introduced. Nevertheless, there are several possibilities extensively discussed in the literature [46]. We found it most convenient to use here the conventional Holstein-Primakoff transformation because it preserves the Hermitian properties of the Hamiltonian. We therefore use

$$S_z = S - a^\dagger a; \quad S^+ = \sqrt{2S - a^\dagger a} \ a; \quad S^- = a^\dagger \sqrt{2S - a^\dagger a} \quad (\text{B2})$$

Substituting this transformation into (B1), expanding the radical, and restricting to only cubic and quartic anharmonic terms, we obtain after some algebra

$$\mathcal{H} = \mathcal{H}_0 + 3JS(\mathcal{H}_2 + \mathcal{H}_3 + \mathcal{H}_4) \quad (\text{B3})$$

where $\mathcal{H}_0 = -\frac{3}{2}JS^2N$ is the classical ground state energy, and other terms are

$$\begin{aligned} \mathcal{H}_2 &= \sum_k A_k a_k^\dagger a_k + \frac{B_k}{2} (a_k^\dagger a_{-k}^\dagger + a_k a_{-k}) \\ \mathcal{H}_4 &= \frac{1}{16S} \sum a_1^\dagger a_2^\dagger a_3 a_4 [4(\nu_{1-3} + \nu_{2-3}) + \nu_1 + \nu_2 + \nu_3 + \nu_4] \\ &\quad - 2 (a_1^\dagger a_2^\dagger a_3^\dagger a_4 + a_4^\dagger a_3 a_2 a_1) (\nu_1 + \nu_2 + \nu_3) \\ \mathcal{H}_3 &= i\sqrt{\frac{3}{8S}} \sum (a_1^\dagger a_2^\dagger a_3 - a_3^\dagger a_2 a_1) (\bar{\nu}_1 + \bar{\nu}_2). \end{aligned} \quad (\text{B4})$$

Here $i \equiv k_i$, and

$$\nu_k = \frac{1}{3} \left(\cos k_x + 2 \cos \frac{k_x}{2} \cos \frac{k_y \sqrt{3}}{2} \right); \quad \bar{\nu}_k = \frac{2}{3} \sin \frac{k_x}{2} \left(\cos \frac{k_x}{2} - \cos \frac{k_y \sqrt{3}}{2} \right). \quad (\text{B5})$$

Finally, A_k and B_k are given by

$$A_k = 1 + \frac{\nu_k}{2}; \quad B_k = -\frac{3}{2}\nu_k \quad (\text{B6})$$

At $S = \infty$, anharmonic terms are absent and \mathcal{H}_1 can be diagonalized by a standard Bogolubov transformation

$$a_k = l_k (c_k + x_k c_{-k}^\dagger) \quad (\text{B7})$$

with

$$l_k = \left(\frac{A_k + E_k}{2E_k} \right)^{1/2} ; \quad x_k = -\frac{B_k}{|B_k|} \left(\frac{A_k - E_k}{A_k + E_k} \right)^{1/2}. \quad (\text{B8})$$

and

$$E_k = (A_k^2 - B_k^2)^{1/2} = ((1 - \nu_k)(1 + 2\nu_k))^{1/2} \quad (\text{B9})$$

The diagonalization yields

$$\mathcal{H}_1 = \sum_k E_k c_k^\dagger c_k \quad (\text{B10})$$

It follows from Eqn. (B9) that the excitation spectrum of the ideal gas of magnons has three zero modes, as it indeed should. Two of these modes are at $k = \pm Q$ where $Q = (4\pi/3, 4\pi/\sqrt{3})$ is the ordering momentum in triangular antiferromagnet, and the third is at $k = 0$ and describes soft fluctuations of total magnetization. The expansion near zero modes gives two spin-wave velocities

$$c_\perp = c_{\pm Q} = \frac{3\sqrt{3}}{2\sqrt{2}} J S a \quad (\text{B11})$$

$$c_\parallel = c_{k=0} = \frac{3\sqrt{3}}{2} J S a \quad (\text{B12})$$

The ratio of the two at $S = \infty$ is $c_\parallel/c_\perp = \sqrt{2}$. This was also obtained in other approaches [26].

The infinite S spin-wave results can be also used to get the first quantum correction to on-site magnetization [47]. Indeed, $\langle a^\dagger a \rangle$ in (B2) is nothing but the density of particles which is finite due to the anomalous term in the quadratic form. From (B7, B8), we have $\langle a_k^\dagger a_k \rangle = (A_k - E_k)/2E_k$, and therefore noninteracting spin waves reduce the sublattice magnetization to

$$\langle S \rangle = S \left(1 - \frac{1}{2S} \sum_k \frac{A_k - E_k}{E_k} \right) = S \left(1 - \frac{0.522}{2S} \right) \quad (\text{B13})$$

We next consider corrections to Eqns (B10) and (B12) due to the interactions between spin-waves. We will follow the same line of reasoning as for square-lattice antiferromagnets. However, the presence of cubic terms makes the analysis considerably more involved.

We start with the spin-wave velocity renormalization.

1. Spin-wave velocity

Our goal is to obtain the leading $1/S$ renormalization of spin-wave excitations. For this we consider first-order self-energy corrections due to quartic anharmonicities and second-order corrections due to cubic anharmonicities (recall that cubic terms have the overall

factor $S^{1/2}$). The corrections due to quartic terms are easy to compute, because to leading order in $1/S$, one can get away with simple one-loop diagrams. Equivalently, one can simply decouple the four-fold term in eq. (B4) by making all possible pair averaging. The quadratic form allows for nonzero normal $\langle a_k^\dagger a_k \rangle$ and anomalous $\langle a_k a_{-k} \rangle$ pair products of Bose particles, and the decoupling changes A_k and B_k to

$$\bar{A}_k = \left(1 + \frac{\nu_k}{2}\right) \left(1 + \frac{1}{2S} - \frac{1}{2S} \sum_p \frac{1}{E_p} \left(1 + \frac{\nu_p}{4} + \nu_p^2\right)\right) - \frac{3}{8S} \sum_p \frac{\nu_p}{E_p} (1 - 4\nu_p) \quad (\text{B14})$$

$$\bar{B}_k = -\frac{3}{2}\nu_k \left(1 + \frac{1}{2S} - \frac{1}{2S} \sum_p \frac{1}{E_p} \left(1 + \frac{\nu_p}{4} - \nu_p^2\right)\right) + \frac{3}{8S} \sum_p \frac{\nu_p}{E_p} \quad (\text{B15})$$

A simple inspection then shows that the renormalized spectrum ($\bar{E}_k = (\bar{A}_k^2 - \bar{B}_k^2)^{1/2}$) still keeps a zero mode at $k = 0$, but acquires a finite gap at $k = \pm Q$:

$$E_Q^2 = -\frac{9}{8S} \sum_p \frac{\nu_p(1 - \nu_p)}{E_p} \quad (\text{B16})$$

This finite gap is indeed an artifact of using only quartic terms, and cubic anharmonicities should restore the correct structure of the spectrum, as we demonstrate below.

There are several ways to deal with the cubic terms: one can either calculate the effective four-fold vertex produced by two triple vertices [48,49], and then use the decoupling procedure, or one can transform to quasiparticles (i.e., diagonalize the quadratic form) considering first only quartic corrections, and then calculate the renormalization of the excitation spectrum due to cubic terms in the second-order perturbation theory. Below we use the second approach which is technically advantageous. We therefore first transform from particle operators (a_k) to quasiparticles (c_k) using eq. (B7), but with \bar{A}_k and \bar{B}_k instead of A_k and B_k . The bare Hamiltonian then keeps the form of eq.(B10) with \bar{E}_k instead of E_k . On the other hand, the structure of cubic vertices becomes more involved after the transformation to quasiparticles, and instead of Eqn. (B4) we obtain

$$\mathcal{H}_3 = i\sqrt{\frac{3}{32S}} \sum c_1^\dagger c_2^\dagger c_3 \Phi_1(1, 2; 3) + \frac{1}{3} c_1^\dagger c_2^\dagger c_3^\dagger \Phi_2(1, 2, 3) + H.c \quad (\text{B17})$$

The vertex functions Φ_1 and Φ_2 are given by

$$\Phi_1(1, 2; 3) = \frac{\tilde{\Phi}_1(1, 2; 3)}{\sqrt{\bar{E}_1 \bar{E}_2 \bar{E}_3}}; \quad \Phi_2(1, 2, 3) = \frac{\tilde{\Phi}_2(1, 2, 3)}{\sqrt{\bar{E}_1 \bar{E}_2 \bar{E}_3}} \quad (\text{B18})$$

where

$$\begin{aligned} \tilde{\Phi}_1(1, 2; 3) &= \bar{\nu}_1 f_-^{(1)} (f_+^{(2)} f_+^{(3)} + f_-^{(2)} f_-^{(3)}) + \bar{\nu}_2 f_-^{(2)} (f_+^{(1)} f_+^{(3)} + f_-^{(1)} f_-^{(3)}) + \bar{\nu}_3 f_-^{(3)} (f_+^{(1)} f_+^{(2)} - f_-^{(1)} f_-^{(2)}) \\ \tilde{\Phi}_2(1, 2, 3) &= \bar{\nu}_1 f_-^{(1)} (f_+^{(2)} f_+^{(3)} - f_-^{(2)} f_-^{(3)}) + \bar{\nu}_2 f_-^{(2)} (f_+^{(1)} f_+^{(3)} - f_-^{(1)} f_-^{(3)}) + \bar{\nu}_3 f_-^{(3)} (f_+^{(1)} f_+^{(2)} - f_-^{(1)} f_-^{(2)}) \end{aligned}$$

and

$$f_{\pm}^{(i)} = (\bar{A}_i \pm \bar{B}_i)^{1/2}. \quad (\text{B19})$$

The self-energy diagrams to order $1/S$ are shown on Fig. 4. We see that cubic terms give rise to both normal and anomalous self-energy parts so that the dispersion relation again has the form typical for a 2×2 problem:

$$(\omega + \Sigma_a(k, \omega))^2 = (\bar{E}_k + \Sigma_s(k, \omega))^2 - (\Sigma_{+,+}(k, \omega))^2 \quad (\text{B20})$$

where $\Sigma_{s,a}(k, \omega) = \frac{1}{2} (\Sigma_{+,-}(k, \omega) \pm \Sigma_{+,-}(-k, -\omega))$. However, it is not difficult to check that $\Sigma_{-,-} \sim \Sigma_{+,+} \sim 1/S$ and therefore anomalous self-energy terms contribute to the excitation energy only to order $1/S^2$, while to order $1/S$ a solution of Eqn (B20) is simply $\omega = \tilde{E}_k$ where

$$\tilde{E}_k^2 = \bar{E}_k^2 + 2\bar{E}_k \Sigma_{+,-}(k, \bar{E}_k) \quad (\text{B21})$$

We therefore need to evaluate here only the normal component of the self-energy. The analytical expression for $\Sigma_{+,-}$ is

$$\Sigma_{+,-}(k, \bar{E}_k) = -\frac{3}{16S} \sum \left(\frac{|\Phi_1(1, 2; k)|^2}{\bar{E}_1 + \bar{E}_2 - \bar{E}_k} + \frac{|\Phi_2(1, 2, k)|^2}{\bar{E}_1 + \bar{E}_2 + \bar{E}_k} \right) \quad (\text{B22})$$

To leading order in $1/S$ we can indeed use nonrenormalized values for A_k, B_k, E_k in the r.h.s. of (B22).

We first demonstrate that \tilde{E}_k has a true zero mode at $k = Q$. For this we need to evaluate $\Sigma_{+,-}(Q, \bar{E}_Q)$. We found the following equality to be quite useful in the calculation

$$\sqrt{3} \bar{\nu}_{q \pm Q/2} = (A_{q \pm Q/2} + B_{q \pm Q/2}) - (A_{q \mp Q/2} - B_{q \mp Q/2}) \quad (\text{B23})$$

Substituting (B23) into the expressions for the vertex functions and using $A_Q = B_Q = 3/4$, we obtain after simple algebra

$$\tilde{\Phi}_1(1, 2; Q) = \tilde{\Phi}_2(1, 2, Q) = \frac{(E_1 + E_2)}{\sqrt{2}} (f_+^{(1)} f_+^{(2)} - f_-^{(1)} f_-^{(2)}) \quad (\text{B24})$$

Substituting, then, the vertex functions into the formula for the self-energy we obtain using (B19)

$$\Sigma_{+,-}(Q, E_Q) = \frac{1}{2E_p} \frac{9}{8S} \sum_p \frac{\nu_p(1 - \nu_p)}{E_p} \quad (\text{B25})$$

Finally, upon substituting this result into Eqn (B21) and using (B16) for \bar{E}_Q , we find that the gap in the excitation spectrum disappears as it should [50].

Our next step is to expand \bar{E}_k and Σ_k near the zero modes, and obtain the corrections to the spin-wave velocities to order $1/S$. The expansion near $k = 0$ is quite straightforward because $\tilde{\Phi}_1(1, 2; k)$ and $\tilde{\Phi}_2(1, 2, k)$ both scale as k at small k , and one can therefore safely neglect E_k in the denominators in (B22). Doing the algebra, we obtain the renormalized spin-wave velocity at $k \approx 0$ in the form

$$\tilde{c}_{\parallel} = c_{\parallel} \left(1 + \frac{1}{2S} - \frac{1}{3S} \sum \frac{Q_k^2}{E_k} \left(\frac{5}{2} - Q_k^2 + \frac{3}{8} (9 - 4Q_k^2) \Lambda_k \right) \right) \quad (\text{B26})$$

where

$$Q_k^2 = \sin^2 \frac{k_x}{2} + \sin^2 \frac{k_x + \sqrt{3}k_y}{4} + \sin^2 \frac{k_x - \sqrt{3}k_y}{4}$$

$$\Lambda_k = -\frac{1}{3} + \left(\sin^4 \frac{k_x}{2} + \sin^4 \frac{k_x + \sqrt{3}k_y}{4} + \sin^4 \frac{k_x - \sqrt{3}k_y}{4} \right) / Q_k^4$$

Numerical intergration then gives

$$\tilde{c}_{\parallel} = c_{\parallel} \left(1 - \frac{0.115}{2S} \right) \quad (\text{B27})$$

The structure of the expansion near $k = \pm Q$ is more involved and we refrain from presenting the analytical expression for the spin-wave velocity. Numerically, we obtained

$$\tilde{c}_{\perp} = c_{\perp} \left(1 + \frac{0.083}{2S} \right) \quad (\text{B28})$$

Comparing (B27) and (B28), we observe that quantum fluctuations tend to diminish the difference between the two spin-wave velocities. This is consistent with our result (2.7) that the relative difference between \tilde{c}_{\perp} and \tilde{c}_{\parallel} should disappear at the quantum-critical point. We will use (B27) and (B28) below and now proceed with the calculations of sublattice magnetization.

2. Sublattice magnetization

We have shown above that to leading order in $1/S$, the correction to sublattice magnetization comes already from noninteracting magnons (Eqn (B13)). Here we obtain the next term in the expansion in $1/S$, which is also the leading $1/S$ correction to the density of particles. We again have to consider both quartic and cubic terms, since they contribute at the same order to $\sum_k \langle a_k^{\dagger} a_k \rangle$. As before, quartic terms only renormalize the coefficients in the quadratic form, and hence change the expression for the density of particles to

$$\sum_k \langle a_k^{\dagger} a_k \rangle = -\frac{1}{2} + \frac{1}{2} \sum_k \frac{\bar{A}_k}{\bar{E}_k} \quad (\text{B29})$$

where \bar{A}_k and \bar{E}_k are given by (B14) and (B15). In explicit form

$$\frac{1}{2} \sum_k \frac{\bar{A}_k}{\bar{E}_k} = \frac{1}{2} \sum_k \frac{1 + \nu_k/2}{E_k} - \frac{9}{32S} \sum_p \frac{\nu_p^2}{E_p} \sum_q \frac{\nu_q}{E_q} - \frac{9}{32S} \sum_p \frac{\nu_p(1 - \nu_p)}{E_p} \sum_q \frac{\nu_q(1 - \nu_q)}{E_q^3} \quad (\text{B30})$$

We see that the very last term behaves near $q = Q$ as $|q - Q|^{-3}$ which makes the integral over q divergent. The divergence is indeed an artificial one and should disappear when we add the contributions of the cubic terms.

To see how cubic terms modify (B29), we express the density of particles in terms of the quasiparticles operators using (B7) and (B8):

$$\sum_k \langle a_k^\dagger a_k \rangle = -\frac{1}{2} + \frac{1}{2} \sum_k \frac{\bar{A}_k}{\bar{E}_k} - \sum_k \frac{\bar{B}_k}{\bar{E}_k} \langle c_k c_{-k} \rangle + \sum_k \frac{\bar{A}_k}{\bar{E}_k} \langle c_k^\dagger c_k \rangle \quad (\text{B31})$$

The first two terms are just the renormalized spin-wave terms. The third correction is related to the anomalous self-energy term in Fig.4. Performing the frequency summation in this term, we obtain

$$- \sum_k \frac{\bar{B}_k}{\bar{E}_k} \langle c_k c_{-k} \rangle = -\frac{9}{32S} \sum_k \frac{\nu_k}{E_k^3} \Psi_k \quad (\text{B32})$$

where

$$\Psi_k = \sum \frac{1}{E_1 E_2} \frac{\tilde{\Phi}_1(1, 2; k) \tilde{\Phi}_2(1, 2, -k)}{E_1 + E_2 + E_k} \quad (\text{B33})$$

Finally, the last term in (B31) contains the density of quasiparticles. This density is finite to order $1/S$ because among cubic non-linearities, there is the term which describes simultaneous emission of three spin-waves. Evaluating the expectation value of $\langle c_k^\dagger c_k \rangle$ by the usual means, we obtain

$$\sum_k \frac{\bar{A}_k}{\bar{E}_k} \langle c_k^\dagger c_k \rangle = \frac{3}{16S} \sum_k \frac{1 + \nu_k/2}{E_k^2} \Upsilon_k \quad (\text{B34})$$

where

$$\Upsilon_k = \sum \frac{1}{E_1 E_2} \frac{|\tilde{\Phi}_2(1, 2, k)|^2}{(E_1 + E_2 + E_k)^2} \quad (\text{B35})$$

We first show that the total expression for the density of particles is free from divergencies. Simple inspection of Eqns (B32) - (B35) shows that the divergent contributions from the cubic terms (namely, $1/E^3$ and $1/E^2$ terms in (B32) and $1/E^2$ terms in (B34)) come from the region $k \approx Q$, where Ψ and Υ tend to constant values. For these k , we again use (B23), substitute it into the vertex functions, and after a simple algebra obtain

$$\Psi_k = -(1 - \nu_Q) \sum_p \frac{\nu_p(1 - \nu_p)}{E_p} - E_k \Upsilon_Q + O(E_k^2) \quad (\text{B36})$$

Substituting further this expression into (B32) and comparing the result with the divergent piece in (B30), we find that the $1/E^3$ contributions from cubic and quartic terms, and the $1/E^2$ contributions from the two cubic terms cancel each other, so that the $1/S$ correction to the density of particles is finite, as it of course should be. We then performed numerical computation of the $1/S$ terms in (B31) and obtained

$$\langle S \rangle = \left(S - 0.261 + \frac{0.027}{(2S)} \right) \quad (\text{B37})$$

For $S = 1/2$, Eqn (B37) yields $\langle S \rangle \approx 0.266$, which is close to half of the classical value. A very similar result was obtained earlier by Miyake [51], who calculated the on-site magnetization to order $1/S^2$ by evaluating numerically the response to a staggered magnetic field. His estimate for the $1/S^2$ correction is however somewhat smaller than ours (0.01 instead of 0.027). In any event, $1/S^2$ terms are rather small and can hardly change substantially the lowest-order spin-wave result for the magnetization [47]. We therefore found no support for the recent claim [9] that the value of magnetization is substantially lower than the spin-wave prediction. Note, in passing, that for square lattice antiferromagnet, the first anharmonic correction to $\langle S \rangle$ is identically zero [52]. Indeed, cubic terms are absent in the square-lattice antiferromagnet, and $1/S$ corrections due to quartic terms do not change the shape of the quasiparticle spectrum (that is, $\bar{A}_k/\bar{E}_k = A_k/E_k$). The next to leading order correction in the square-lattice case has been calculated and found to be very small [52].

3. Uniform susceptibility

Now we calculate, to order $1/S$, the response of a triangular antiferromagnet to an external magnetic field. We have already discussed in Sec.III that the magnetic susceptibility tensor in a triangular antiferromagnet has the form [23]

$$\chi_{\alpha\beta} = \chi_{\perp} \delta_{\alpha\beta} + (\chi_{\parallel} - \chi_{\perp}) m_{\alpha} m_{\beta} \quad (\text{B38})$$

where \mathbf{m} is a unit vector which specifies the plane of spin ordering. This form of $\chi_{\alpha\beta}$ implies that the ordered state should have two different spin susceptibilities. They can be viewed as the response to the field applied perpendicular to the plane of spin ordering, i.e., along \vec{m} (χ_{\parallel}), and as the response to a field directed in the plane (χ_{\perp}). In the latter case, we need to introduce an infinitesimally small anisotropy which keeps the spins in the basal plane.

For classical spins, the transverse and longitudinal susceptibilities can easily be obtained by minimizing the ground state energy. This yields $\chi_{\perp} = \chi_{\parallel} = 2/9\sqrt{3}Ja^2$ where a is the interatomic spacing ($a^2\sqrt{3}/2$ is the unit cell volume). As in the bulk of the paper, we define χ_{\perp} and χ_{\parallel} without the gyromagnetic ratio $g\mu_B/\hbar$. We see that the two susceptibilities are equal in the classical limit [53]. This degeneracy in the response to a magnetic field in a 2D triangular antiferromagnet has attracted some attention in the past as an example of the "order from disorder" phenomenon [53,54,55,56,57]. For our present purposes, it is sufficient to observe that the degeneracy is a purely classical effect. It is not related to the symmetry properties of a quantum system and therefore should be broken by quantum fluctuations.

Technically, the computations in a finite field are more involved because the transverse field breaks the 120° ordering in the basal plane. In this case, a transformation to a twisted coordinate frame is no longer advantageous because umklapp processes also contribute to order $1/S$. It is then more convenient to introduce a separate bose field for each of three sublattices. For the longitudinal response, the 120° ordering in the basal plane is preserved and a one-sublattice description with no umklapp terms is still valid. However, one has to be careful in this case as well, because in the presence of a field, the excitation spectrum is no longer an even function of k . This is consistent with the fact that time reversal symmetry in a magnetic field requires that in changing $k \rightarrow -k$ in the spectrum, one has to change simultaneously the sign of H .

The corrections to the susceptibility tensor to order $1/S$ were computed by Golosov and one of us [56]. We refrain from presenting the details of the calculations and list here only the results. To order $1/S$, they are (notice that the definitions of χ_\perp and χ_\parallel in [56] are interchanged compared to ours):

$$\chi_\perp = \frac{2}{9\sqrt{3}Ja^2} Z_\perp^\chi; \quad \chi_\parallel = \frac{2}{9\sqrt{3}Ja^2} Z_\parallel^\chi \quad (\text{B39})$$

where

$$Z_\parallel^\chi = \left(1 - \frac{1}{2S} \sum_k \frac{\nu_k(1-\nu_k)}{E_k} \right) = 1 - \frac{0.448}{2S}. \quad (\text{B40})$$

and

$$Z_\perp^\chi = \left(1 - \frac{1}{2S} \sum_k \frac{\nu_k(1+2\nu_k)}{E_k} + \frac{3}{2S} \sum_k \frac{\nu_k^2}{E_{k_1} + E_{k_2}} \frac{f_-^{(1)} f_-^{(2)}}{E_{k_1} E_{k_2}} \right) = 1 - \frac{0.291}{2S}. \quad (\text{B41})$$

where $f^{(i)} \equiv f^{(k_i)}$ were defined in (B19). Note that contrary to the situation in a stacked $3d$ triangular antiferromagnet where $\chi_\parallel > \chi_\perp$, the transverse (in-plane) susceptibility in the $2d$ case turns out to be larger than the longitudinal one; this gives rise to an unconventional phase diagram in a magnetic field which has been discussed several times in the literature [53,54,55,56].

4. Spin stiffness

With the values of the two spin-wave velocities and spin susceptibilities at hand, we are now in a position to calculate the spin stiffnesses. To order $1/S$ they are

$$\rho_\perp = \chi_\perp c_\perp^2 = \frac{\sqrt{3}}{4} JS^2 Z_\perp^\rho \quad \rho_\parallel = \chi_\parallel c_\parallel^2 = \frac{\sqrt{3}}{2} JS^2 Z_\parallel^\rho \quad (\text{B42})$$

where

$$Z_\perp^\rho = 1 - 0.125/2S, \quad Z_\parallel^\rho = 1 - 0.678/2S \quad (\text{B43})$$

Finally, substituting the results (B39)- (B42) into (2.6), we obtain for $N = 2$

$$\rho_s = \frac{1 - 0.402/2S}{\sqrt{3}} JS^2, \quad \chi = \frac{2}{9\sqrt{3}Ja^2} (1 - 0.343/2S) \quad (\text{B44})$$

APPENDIX C: COMPUTATIONS IN THE NÉEL STATE AT $T = 0$

In this Appendix, we derive to order $1/N$, the expression for $T = 0$ sublattice magnetization near the quantum phase transition. This result will be used in the derivation of

the universal scaling forms for uniform and staggered susceptibilities in both renormalized-classical and quantum-critical regions. We also reproduce the $1/N$ expressions for the relative difference between longitudinal and transverse spin-stiffness and spin susceptibility which were obtained by other means in Sec III.

Our point of departure is the functional integral for the $SU(N) \times U(1)$ σ -model, Eqn (2.1). At $T = 0$, the spin-rotation symmetry is broken, and we represent the N component complex vector z of length N as

$$z = (\sigma_0 + i\sigma_1, \pi_1 + i\pi_2, \pi_3 + i\pi_4 \dots), \quad (\text{C1})$$

where $\langle \sigma_0 \rangle$ is finite. This parametrization slightly differs from (3.8), in that σ_1 and π_i are defined without a factor $1/2$; notice also that we do not neglect fluctuations in the direction of the condensate. Upon substituting (C1) into (2.1), the functional integral becomes

$$\mathcal{Z} = \int \mathcal{D}\sigma_0 \mathcal{D}\sigma_1 \mathcal{D}\pi_l \delta(\sigma_0^2 + \sigma_1^2 + \pi_l^2 - N) e^{-\mathcal{S}} \quad (\text{C2})$$

where

$$\begin{aligned} \mathcal{S} = & \int d^2r \int_0^\infty d\tau \sum_{\mu=\bar{x},t} \sum_{l,m} \frac{1}{g_\mu} \left((\partial_\mu \sigma_0)^2 + (\partial_\mu \sigma_1)^2 + (\partial_\mu \pi_l)^2 \right) + \\ & \frac{\gamma_\mu}{Ng_\mu} (\sigma_0 \partial_\mu \sigma_1 - \sigma_1 \partial_\mu \sigma_0 \pi_{2m} \partial_\mu \pi_{2m+1} - \pi_{2m+1} \partial_{mu} \pi_{2m})^2, \end{aligned} \quad (\text{C3})$$

where the indices l and m run from 1 to $2N - 2$ and from 1 to $N - 1$. The values of the couplings are the same as in (2.3). As in the body of the paper, we focus on the situation near the zero-temperature phase transition, which generally occurs at some $g = g_c(\gamma_\mu)$. We also assume that the anisotropy is small, and make all computations to leading order in γ only.

The large N expansion proceeds along the same lines as for square-lattice antiferromagnets [25]. We introduce the condensate value, σ , via

$$\sigma_0 = \sqrt{N}\sigma + \tilde{\sigma}_0 \quad (\text{C4})$$

and impose the constraint by introducing the Lagrange multiplier λ into the functional integral. At $N = \infty$, the saddle-point equation gives

$$\sigma^2 = \frac{g_c - g}{g_c}, \quad (\text{C5})$$

where g_c is the same as in the isotropic case.

We first consider how the ratio of the stiffnesses scales with $g - g_c$. For this we observe that the only anisotropic piece in (C3) which survives at infinite N is $(\gamma_\mu/2g_\mu) \sigma^2 (\partial_\mu \sigma_1)^2$. Hence, at $N = \infty$, the propagators for π fields remain the same as in the isotropic $O(2N)$ model

$$G_\pi = \frac{g_\tau}{2} \frac{1}{\omega_n^2 + c_0^2 k^2}, \quad (\text{C6})$$

while the propagator for the σ_1 field acquires a correction linear in γ_μ

$$G_{\sigma_1} = \frac{g_\tau}{2} \frac{1}{(1 + \gamma_\tau \sigma^2) \omega_n^2 + (1 + \gamma_x \sigma^2) c_0^2 k^2} \quad (\text{C7})$$

where $c_0 = \sqrt{\rho_\perp^0 / \chi_\perp^0}$. Eqns (C6) and (C7) identify (upto an overall factor) G_π and G_{σ_1} as the transverse and longitudinal propagators of gapless spin-wave excitations in the ordered state. Each of the propagators can now be reexpressed in terms of the fully renormalized spin-stiffness and spin susceptibility by collecting γ -independent terms, which are the same for both propagators. Comparing then the two expressions, we obtain

$$\frac{\rho_\parallel - \rho_\perp}{\rho_\perp} = \gamma_x \sigma^2 \quad \frac{\chi_\parallel - \chi_\perp}{\chi_\perp} = \gamma_\tau \sigma^2 \quad (\text{C8})$$

where ρ and χ are now fully renormalized $T = 0$ spin-stiffness and spin susceptibility respectively. We see from (C8) that while the relative difference of the bare stiffnesses is γ_μ , the ratio of the renormalized stiffnesses contains the extra factor σ^2 and therefore tends to zero as the system approaches quantum phase transition point. We now introduce the crossover exponents ϕ_1 and ϕ_2 in the same way as in Sec II. Namely, we decompose γ_μ into their trace and traceless parts as

$$\gamma_x = \gamma_1 + \gamma_2 \quad \gamma_\tau = \gamma_1 - 2\gamma_2 \quad (\text{C9})$$

and define ϕ_1 and ϕ_2 as

$$\begin{aligned} \frac{\rho_\parallel - \rho_\perp}{\rho_\perp} &= \gamma_1 (\xi_J)^{-\phi_1} + \gamma_2 (\xi_J)^{-\phi_2} \\ \frac{\chi_\parallel - \chi_\perp}{\chi_\perp} &= \gamma_1 (\xi_J)^{-\phi_1} - 2\gamma_2 (\xi_J)^{-\phi_2} \end{aligned} \quad (\text{C10})$$

where ξ_J is the Josephson correlation length measured in lattice units. As g approaches g_c , ξ_J behaves as $\xi_J \sim (1 - g_x/g_c)^{-\nu}$. At $N = \infty$, $\nu = 1$. Using (C5), we then obtain $\phi_1 = \phi_2 = 1$.

Our next step will be to calculate the $1/N$ corrections to the crossover exponents. The corresponding diagrams are presented in Fig 5. It is not difficult to show that the polarization operator at $T = 0$, $\Pi^*(k, i\omega)$, has no γ -dependent corrections to the leading order in $1/N$ and we therefore can use the same expression as in the isotropic case [25]:

$$\Pi^*(k, i\omega) = \frac{\hbar c_0^2}{8\sqrt{c_0^2 k^2 + \omega^2}} + \frac{2}{g_\tau} \langle \sigma \rangle^2 \frac{1}{c_0^2 k^2 + \omega^2} \quad (\text{C11})$$

We will also need the expression for the propagator for the fluctuating component of the field along the direction of the condensate:

$$G_{\tilde{\sigma}_0} = \frac{g_\tau}{2} \frac{1}{\omega_n^2 + c_0^2 k^2}, \left(1 - \frac{2}{g} \langle \sigma \rangle^2 \frac{1}{\Pi^*(k, i\omega)} \frac{1}{\omega_n^2 + c_0^2 k^2} \right), \quad (\text{C12})$$

and expressions for $\langle \sigma \rangle^2$ and ξ_J with logarithmic accuracy to order $1/N$:

$$\begin{aligned}\langle\sigma\rangle^2 &= \left(\frac{g_c - g}{g_c}\right) \left(1 + \frac{4}{\pi^2 N} \log \frac{g_c}{g_c - g}\right) \\ \xi_J^{-1} &= \left(\frac{g_c - g}{g_c}\right) \left(1 + \frac{16}{3\pi^2 N} \log \frac{g_c}{g_c - g}\right).\end{aligned}\tag{C13}$$

The evaluation of the diagrams is now straightforward. Collecting the contributions from all diagrams on Fig. 5 and restricting to only logarithmic contributions to order $1/N$, we obtain after some algebra

$$\begin{aligned}\frac{\rho_{\parallel} - \rho_{\perp}}{\rho_{\perp}} &= \frac{g_c - g}{g_c} \left[\gamma_x \left(1 + \frac{64L}{15\pi^2 N}\right) + \gamma_{\tau} \frac{16L}{15\pi^2 N} \right] \\ \frac{\chi_{\parallel} - \chi_{\perp}}{\chi_{\perp}} &= \frac{g_c - g}{g_c} \left[\gamma_{\tau} \left(1 + \frac{16L}{5\pi^2 N}\right) + \gamma_x \frac{32L}{15\pi^2 N} \right]\end{aligned}\tag{C14}$$

where $L = \log(1 - g/g_c)$. We then use (C9) and find

$$\phi_1 = 1 + \frac{112}{15\pi^2 N} \quad \phi_2 = 1 + \frac{32}{3\pi^2 N}\tag{C15}$$

These values for the crossover exponents coincide with Eqn (2.8) obtained by other means in Sec. II

Our next move will be to compute, in the $1/N$ expansion, the critical exponent for the order parameter. Using the definition (1.12) and Eqns (C1) and (C4), we obtain

$$N_0 = SZ_S \left[\left(\langle\sigma\rangle^2 + \frac{1}{N} \langle\tilde{\sigma}_0\rangle^2 \right) + \mathcal{O}\left(\frac{1}{N}\right) \right]\tag{C16}$$

where $\mathcal{O}(1/N)$ stands for *regular* $1/N$ corrections from the other components of z -field which can be neglected in the calculations of the critical exponents. Using then (C12) we find

$$N_0 = SZ_S \langle\sigma\rangle^2 \left(1 - \frac{2}{g} \int \frac{1}{\Pi^*(k, i\omega)} \frac{1}{\omega_n^2 + c_0^2 k^2} \right).\tag{C17}$$

Performing the integration with the logarithmic accuracy and exponentiating the result, we obtain

$$N_0 = SZ_S \langle\sigma\rangle^{\varepsilon}\tag{C18}$$

where

$$\varepsilon = 1 + \frac{4}{N\pi^2}.\tag{C19}$$

Expressing now $\langle\sigma\rangle$ in a conventional way as $\langle\sigma\rangle^2 = (\Delta g/g_c)^{\beta}$, where $\beta = 1 - 4/N\pi^2$, we find $N_0 \sim (\Delta g/g_c)^{\bar{\beta}}$, where

$$\bar{\beta} = 1 + \mathcal{O}\left(\frac{1}{N^2}\right)\tag{C20}$$

We will also need the $1/N$ result for the staggered spin susceptibility at $T = 0$. Using (1.11), (C1), (C4) and the result obtained in Section IV that the number of transverse spin-wave modes in the ordered state is $N_{sw} = 2N$, we find that the transverse spin susceptibility at $N = \infty$ and $k \ll \xi_J^{-1}$ is related to the propagator of the z -field

$$\chi_s^{bb}(k, i\omega) = \frac{(SZ_s)^2 \langle \sigma \rangle^2}{2\rho_\perp^0} \frac{1}{k^2 + \omega^2/c_0^2}. \quad (\text{C21})$$

where index b labels transverse spin components. The relevant $1/N$ corrections are now the same as in collinear antiferromagnets. Using the results of Ref [25], we find that they can be completely absorbed into the renormalization of N_0 and ρ_\perp . Assuming, as in the bulk of the paper, that the anisotropic term in the action will transform ρ_\perp and c_\perp into ρ_s and c given by (4.6), we obtain

$$\chi_s^{bb}(k, i\omega) = \frac{N_0^2}{2\rho_s} \frac{1}{k^2 + \omega^2/c^2}. \quad (\text{C22})$$

Finally, we calculate in $1/N$ expansion, the critical exponent $\bar{\eta}$. For this, we consider the behavior of dynamical spin susceptibility at $T = 0$ right at the transition point, $g = g_c$. At this point $\langle \sigma \rangle = 0$, and the spin-spin correlation function is again related to the polarization operator of z -fields. At $N = \infty$ and $g = g_c$, the polarization operator is given by the first term in (C11). To first order in $1/N$, we have to consider both self-energy and vertex corrections in the polarization bubble (Fig 3). They both contain logarithms of external momentum. Evaluating the diagrams in Fig 3 with logarithmical accuracy, we obtain:

$$\Pi^*(k, i\omega) = \frac{A_N}{(c\Lambda)^{2\mu}} \frac{c^2}{8(c^2k^2 + \omega^2)^{1-\bar{\eta}/2}} \quad (\text{C23})$$

where $A_N = 1 + O(1/N)$, and

$$\bar{\eta} = 1 + \frac{32}{3\pi^2 N}. \quad (\text{C24})$$

REFERENCES

- [1] V. Kalmeyer and R.B. Laughlin, Phys. Rev. Lett., **59**, 2095 (1987); X.G. Wen, F. Wilczek and A. Zee, Phys. Rev. B **39**, 11413 (1989).
- [2] N. Read and S. Sachdev, Phys. Rev. Lett. **62**, 1694 (1989); *ibid* **42**, 4568 (1990); Phys. Rev. Lett. **66**, 1773 (1991); S. Sachdev and N. Read, Int. J. Mod. Phys. **B5**, 219 (1991).
- [3] K. Yang, L.K. Warman and S.M. Girvin, Phys. Rev. Lett. **70**, 2641 (1993).
- [4] D.P. Arovas and D. Auerbach, Phys. Rev. B **38**, 316 (1988); Phys. Rev. Lett. **61**, 617 (1988).
- [5] For a recent review see e.g. A. Harrison, in "Annual Reports on the Progress of Chemistry (Royal Soc. of Chemistry, UK), **87A**, 211, (1992); **88A**, 447, (1992) and M.L. Plumer, A. Caille, A. Mailhot and H.T. Diep, to appear in 'Magnetic Systems with competing interactions', H.T. Diep ed., World Scientific (1994).
- [6] P. Fazekas and P.W. Anderson, Philos. Mag. **30**, 432 (1974).
- [7] S. Miyashita, J. Phys. Soc. Jpn. **53**, 44 (1984); B. Bernu, C. Lhuillier and L. Pierre, Phys. Rev. Lett. **69**, 2590 (1992); P. Azaria, B. Delamott and D. Mouhanna, Phys. Rev. Lett., **70**, 2483 (1993). Several numerical studies however predicted the absence of long-range order for $S = 1/2$: see e.g. H. Nishimori and H. Nakanishi, J. Phys. Soc. Jpn, **57**, 626 (1988) and references therein.
- [8] D.A. Huse and V. Elser, Phys. Rev. Lett. **60**, 2531 (1988).
- [9] R.R.P. Singh and D. Huse, Phys. Rev. Lett. **68**, 1706 (1992).
- [10] V. Elser, Phys. Rev. Lett., **62**, 2405 (1990).
- [11] A.P. Ramirez, G.P. Espinosa, and A.S. Cooper, Phys. Rev. Lett. **64**, 2070 (1990) C. Broholm, G. Aeppli, G.P. Espinosa, and A.S. Cooper, Phys. Rev. Lett. **65**, 3173 (1991).
- [12] S. Sachdev, Phys. Rev. B **45**, 12377 (1992).
- [13] P. Chandra, P. Coleman and I. Ritchey, Phys. Rev. B. to appear
- [14] J. Villain, R. Bidaux, J.P. Curton and R. Conte, J. Physique **41**, 1263 (1980).
- [15] A.B. Harris, C. Kallin and A.J. Berlinsky, Phys. Rev B **45**, 2889 (1992); J.T. Chalker, P.S. Holdsworth and E.F. Shender, Phys. Rev. Lett. **68**, 855 (1992); A.V. Chubukov, Phys. Rev. Lett. **69**, 832 (1992); J.N. Reimers, A.J. Berlinsky and A.-C Shi, Phys. Rev. B **43**, 865 (1991); D.L. Huber and W.Y. Cheong, Phys. Rev. B **47**, 3220 (1993).
- [16] J.von Delft and C.L. Henley, Phys. Rev. Lett., **69**, 3236 (1992); A. Chubukov, J. Appl. Phys. **73**, 5639 (1993).
- [17] L.B. Ioffe and A.I. Larkin, Int. J. Mod. Phys, B **2**, 203 (1988); P. Chandra, P. Coleman and A.I. Larkin, J. Phys. Condens. Matter **2**, 7933 (1990); A.V. Chubukov, Phys. Rev. B **44**, 392 (1991); F. Mila, D. Poliblanco and C. Bruder, Phys. Rev. B **43**, 7891 (1991); M. Gelfand, Phys. Rev. B **42**, 8206 (1990); J. Ferrer, Phys. Rev. B **47**, 8769 (1993); J. Richter, Phys. Rev. B **47**, 5794 (1993); N.B. Ivanov and J. Richter, Phys. Rev. B., to appear.
- [18] P. Azaria, B. Delamott, and T. Jolicoeur, Phys. Rev. Lett. **64**, 3175 (1990); P. Azaria, B. Delamott and D. Mouhanna, Phys. Rev. Lett **68**, 1762 (1992).
- [19] A.M. Polyakov, Phys. Lett **59** , 79 (1975).
- [20] S.M. Hayden, G. Aeppli, H. Mook, D. Rytz, M.F. Hundley and Z. Fisk, Phys. Rev. Lett **66**, 821 (1991); B. Keimer, N.Belk, R.J. Birgeneau, A. Cassanho, C.Y. Chen, M. Greven,

- M.A. Kastner and G. Shirane, *Rhys. Rev. B* **46**, 14034 (1992); T. Imai, C.P. Slichter, K. Yoshimura and K. Kosuge, *Phys. Rev. Lett.*, **70**, 10002 (1993).
- [21] see e.g. E. Manousakis *Rev. Mod. Phys.* **63**, 1 (1991) and references therein.
- [22] S. Sachdev, in *Low Dimensional Quantum Field Theories for Condensed Matter Physicists*, Proceedings of the Trieste Summer School 1992, World Scientific, to be published, and references therein. Available as paper 9303014 on cond-mat@babbage.sissa.it.
- [23] A.F. Andreev and V. I. Marchenko, *Sov. Phys. Usp.* **23**, 21, (1980).
- [24] B.I. Halperin and W.M. Saslow, *Phys. Rev. B* **16**, 2154 (1977)
- [25] A. Chubukov, S. Sachdev and Jinwu Ye, *Phys. Rev. B*, in press; S. Sachdev and Jinwu Ye, *Phys. Rev. Lett.* **69**, 2411 (1992); A.V. Chubukov and S. Sachdev, *Phys. Rev. Lett.* **71**, 169 (1993).
- [26] T. Dombre and N. Read, *Phys. Rev B* **39**, 6797 (1989).
- [27] T. Garel and P. Pfeuty, *J. Phys C* **9**, 743 (1976); D. Bailin, A. Love and M.A. Moore, *J. Phys. C* **10**, 1159 (1977); for a review article see M.L. Plumer and A. Caille, *J. Appl. Phys.* **70**, 5961 (1991).
- [28] H. Kawamura, *Phys. Rev. B* **38**, 4916 (1988).
- [29] P. Azaria, B. Delamott, F. Delduc and T. Jolicoeur, *Nucl. Phys. B* **408**, 485 (1993).
- [30] T. Bhattacharya, A. Billoire, R. Lacaze and T. Jolicoeur, Saclay preprint T93/015.
- [31] H. Kawamura and S. Miyashita, *J. Phys. Sos. Jpn.* **53**, 4138 (1984)
- [32] N. Read, private communication.
- [33] A.M. Polyakov, *Gauge Fields and Strings*, Harwood, New York (1987).
- [34] K. Lang and W. Ruhl, *Z. Phys. C* **51**, 127 (1991).
- [35] S. Chakravarty, B.I. Halperin and D.R. Nelson, *Phys. Rev. Lett.* **60**, 1057 (1988); *Phys. Rev. B* **39**, 2344 (1989).
- [36] P. Hasenfratz, M. Maggiore and F. Niedermayer, *Phys. Lett. B* **245**, 522 (1990); P. Hasenfratz and F. Niedermayer, *Phys. Lett. B* **245**, 529 (1990).
- [37] S. Tyc and B.I. Halperin, *Phys. Rev. B* **42**, 2096 (1990).
- [38] S. Sachdev, *Phys. Lett B* **309**, 285 (1993).
- [39] S. Chakravarty and R. Orbach, *Phys. Rev. Lett* **64**, 224 (1990).
- [40] N. Elstner, R.R.P. Singh and A.P. Young, *Phys. Rev. Lett.*, **71**, 1629 (1993).
- [41] R.R.P. Singh and M. Gelfand, *Phys. Rev. B* **42**, 966 (1990).
- [42] H.Q. Ding and M. Makivic, *Phys. Rev. Lett*, **64**, 1449 (1990); *Phys. Rev. B* **43**, 3662 (1990).
- [43] C.M. Canali, S.M. Girvin and M. Wallin, *Phys. Rev. B* **45**, 10131 (1992).
- [44] J. Igarashi, *Phys. Rev. B* **46**, 10763 (1992).
- [45] R.R.P. Singh, *Phys. Rev. B* **39**, 9760 (1989); see also R.R.P. Singh and D. Huse, *Phys. Rev. B* **40**, 7247 (1989).
- [46] M.I. Kaganov and A.V. Chubukov, *Usp. Fiz. Nauk* **153**, 537 (1987) [*Sov. Phys. Usp.* **30**, 1015 (1987)]; in "Spin Waves and Magnetic Dielectrics" eds. A.S. Borovik-Romanov and S.K. Sinha, Elsevier Science Publ. (1988).
- [47] T. Jolicoeur and J.C. Le Guillou, *Phys. Rev. B* **40**, 2227 (1989).
- [48] E. Rastelli, L. Reatto and A. Tassi, *J. Phys.C* **18**, 353 (1985)
- [49] A.V. Chubukov, *Phys. Rev.* **44**, 5362 (1991).
- [50] Numerical proof that the gap at $k = \pm Q$ is absent was first given in [48]. Analytically, this was first shown in [49] in a way different from the one presented here.

- [51] S.J. Miyake, J. Phys. Sos. Jpn., **61**, 983 (1992).
- [52] G. E. Castilla and S. Chakravarty, Phys. Rev. B **43**, 13687 (1991).
- [53] H. Kawamura and S. Miyashita, J. Phys. Sos. Jpn., **54**, 4530 (1985).
- [54] S.E. Korshunov, J. Phys. C: Solid State Phys. **19**, 5927 (1986).
- [55] B. Kleine, E. Muller-Hartmann, K. Frahm and P. Fazekas, Z. Phys. B **87**, 103 (1992).
- [56] A.V. Chubukov and D. Golosov, J. Phys. Condens. Matter, **3**, 69 (1991).
- [57] Qing Sheng and C.L. Henley J. Phys. Condens. Matter, **4**, 2937 (1992).

FIGURES

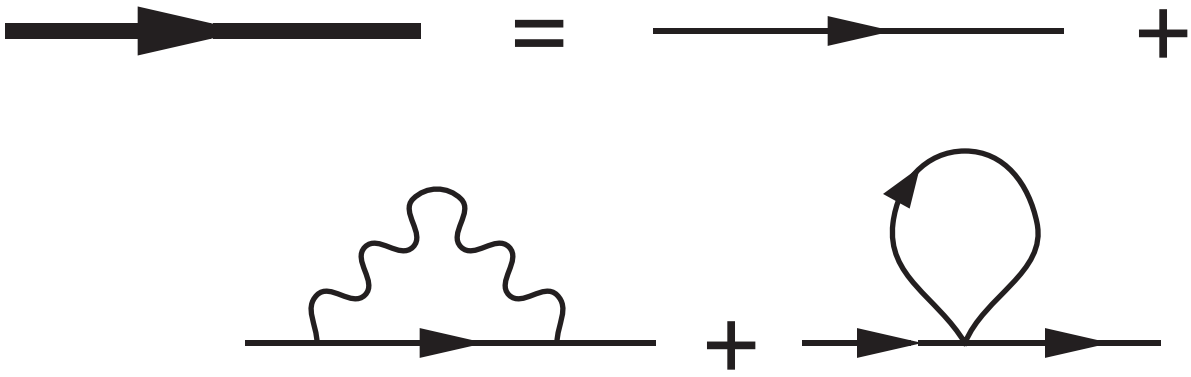
FIG. 1. a. Self-energy corrections to spinon propagator. The heavy solid line is a full spinon propagator, and the wavy line is an inverse polarization operator for spinons. The analytical expression for the vertex is given by (3.17). b. Diagrams which contribute to current-current correlation functions $\langle K_\mu^a K_\mu^b \rangle$ and $\langle J_\mu J_\mu \rangle$ to first order in $1/N$ and to first order in γ_μ . The side vertices (shaded) in the bubbles are $2T^{ab}k_\mu(1 + \gamma_\mu)/g_\mu$ for $U(1)$ response and $2\delta^{ab}k_\mu(1 + \gamma_\mu/N)/g_\mu$ for $SU(N)$ response.

FIG. 2. Diagrams which contribute to renormalization of the Γ vertex (3.17) to order $1/N$.

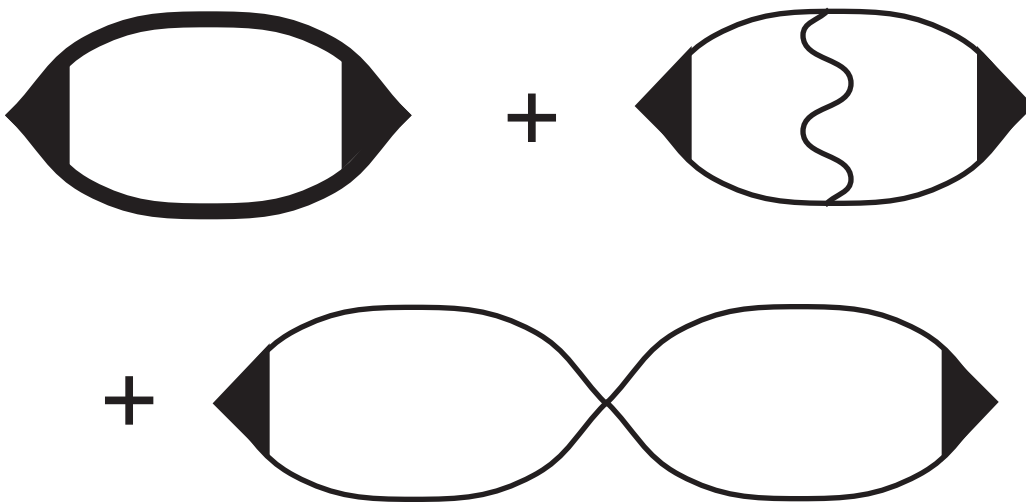
FIG. 3. Diagrams which contribute to the renormalization of the polarization operator to first order in $1/N$ at $\gamma_\mu = 0$. As in Fig.1, heavy solid lines are full spinon propagators.

FIG. 4. Second-order self-energy corrections to magnon propagators due to cubic vertices. Notice that cubic terms always produce anomalous self-energy terms.

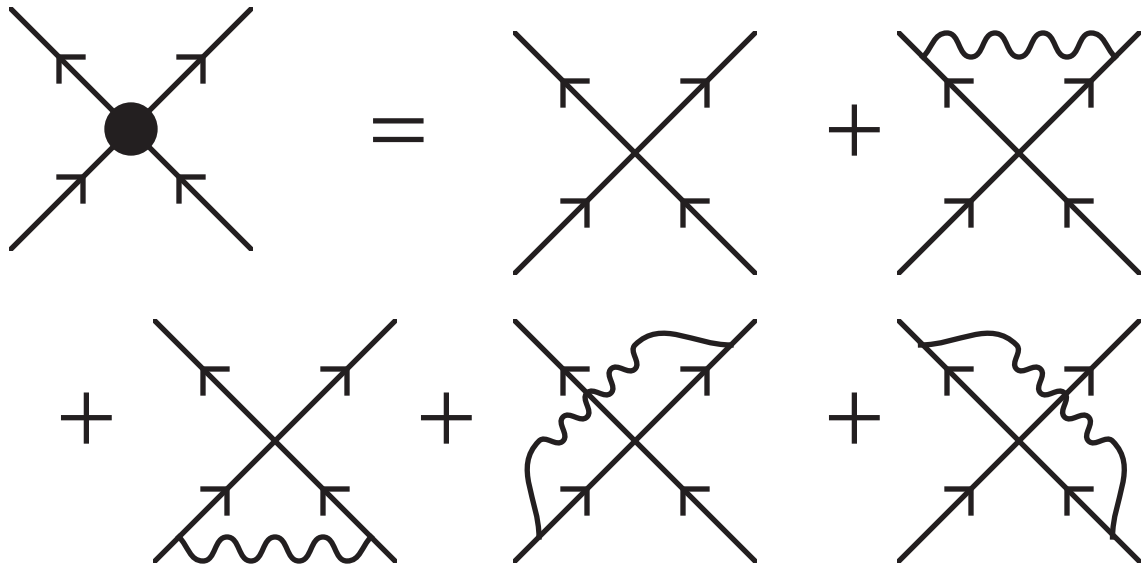
FIG. 5. Self-energy diagrams to order $1/N$ for the propagator of σ_1 field in the ordered state at $T = 0$. Solid line is the propagator of σ_1 given by (C7), dashed line represents the condensate σ , wavy line is inverse polarization operator, and heavy solid line is the propagator of $\tilde{\sigma}_0$ field introduced in (C4): $G_{\tilde{\sigma}_0} = G_\pi(1 - (2/g_\tau)\sigma^2 G_\pi/\Pi^*)$, where G_π is given by (C6).



(a)



(b)



$$\Pi = \text{[thick lens shape]} + \text{[thin lens shape with wavy line]}$$

$$\Sigma_{+-} = \text{Diagram 1} + \text{Diagram 2}$$

The first diagram shows an incoming line from the left that splits into two paths. The upper path curves upwards and then back down to the right, with an arrow pointing left. The lower path curves downwards and then back up to the right, with an arrow pointing left. These two paths recombine into a single line that continues to the right. This is followed by a plus sign and a second diagram. The second diagram is identical to the first, but the arrows on the curved paths point to the right.

$$\Sigma_{++} = \text{Diagram 3} + \text{Diagram 4}$$

The first diagram shows an incoming line from the left that splits into two paths. The upper path curves upwards and then back down to the right, with an arrow pointing left. The lower path curves downwards and then back up to the right, with an arrow pointing left. These two paths recombine into a single line that continues to the right. This is followed by a plus sign and a second diagram. The second diagram is identical to the first, but the arrows on the curved paths point to the right.

$$\Sigma = \text{[Diagram 1]} + \text{[Diagram 2]} + \text{[Diagram 3]} + \text{[Diagram 4]} + \text{[Diagram 5]} + \text{[Diagram 6]}$$

The image shows a mathematical equation for the self-energy Σ in a quantum field theory context. The equation is:

$$\Sigma = \text{[Diagram 1]} + \text{[Diagram 2]} + \text{[Diagram 3]} + \text{[Diagram 4]} + \text{[Diagram 5]} + \text{[Diagram 6]}$$
 The diagrams are arranged in two columns. The left column contains diagrams 1, 3, and 5. The right column contains diagrams 2, 4, and 6.

- Diagram 1:** A horizontal solid line with a wavy loop on top.
- Diagram 2:** A horizontal solid line with two dashed lines meeting at a vertex above it.
- Diagram 3:** A horizontal solid line with a wavy loop on top and two dashed lines meeting at a vertex below it.
- Diagram 4:** A horizontal solid line with two thick diagonal lines meeting at a vertex above it, and a wavy loop on top.
- Diagram 5:** A horizontal solid line with two thick diagonal lines meeting at a vertex below it, and a wavy loop on top.
- Diagram 6:** A horizontal solid line with two thick diagonal lines meeting at a vertex above it, and a wavy loop on the left side.